IN-SITU BLOCKAGE MONITORING OF SENSING LINE

By

AIJAZ AHMED

NUST201260259MRCMS64012F

Research Centre for Modeling & Simulation

National University of Sciences & Technology

2015

IN-SITU BLOCKAGE MONITORING OF SENSING LINE

By

Aijaz Ahmed

A thesis submitted in partial fulfillment of the requirement for the

degree of Masters in Computational Science and Engineering

Research Centre for Modeling & Simulation

National University of Sciences & Technology

2015

<u>STATEMENT OF ORIGINALITY</u>

I hereby certify that the work embodied in this thesis is the result of original research
and has not been submitted for a higher degree to any other University or Institution.

Date	AIJAZ AHMED

Dedication

This work is dedicated to my parents, my family and to persons who live to

serve the humanity.

Acknowledgements

"Recite in the name of your Lord who created - Created man from a clinging substance. Recite and your Lord is the most Generous - Who taught by the pen - Taught man that which he knew not."   The QURAN, Sura Al-Alaq 96/1-5

First, and foremost, I praise the glory of ultimate power, the great God, Who extended his help to get through this research, degree and thesis. I am thankful to my supervisor Dr.Syed Salman Shahid for his continuous support and guidance. I think without his supervision, it would not been possible to complete this thesis. Let me also offer my thanks to Engr. Sikander Hayat Mirza,,who has craft to infuse the love for knowledge and research among his students, his advices made my work easier. Dr.Adan Maqsood and Mr.Muhammad Tariq Saeed also provided me valuable suggestions. I am grateful to them.

My friends and colleagues Mohammad Ali Awan and Muhammad Alamgeer extended their hands of cooperation during my research work. My thanks go to them as well. I am indebted to my family as well for help, specially my wife, she herself is an Electronics Engineer, flanked me during this effort.

Abstract

Nuclear Power is expected to release low Green House Gas (GHG) emissions with very low impact upon climate change. It emits usually 6-10 g CO_2/KWHe. Major share of nuclear power in energy mix can actively contribute in the reduction of GHG-emissions.It is considered that uranium cost is much lower, when compared fossil fuels.Nuclear power is inexpensive source of energy. Over the last 30 years, nuclear power plants around the globe have demonstrated their capacity and capability to produce base-load at affordable price. The nuclear power price does not fluctuate as of conventional fossil fuels. An other option for power generation are renewable energy sources which are under consideration in many countries around the world, but owing to their limited production capacity and weather dependency make their installation/operation at limited scale and their share in energy mix policy is very low.

Uranium resources are widely distributed across the globe; however fossil fuel resources are accumulated in few regions of the world. It is very likely that uranium mining will not yield tensions and crisis among nations as it has been case for the gas and oil. Because of these factors, it is widely believed that nuclear power is a viable source of energy to meet future demands. There are pros and cons of nuclear power. Nuclear power plants (NPPs) requires strict monitoring of the physical parameters, e.g. Neutron flux, temperature of the reactor coolant, Reactor water level etc. If these parameters are not maintained within limits, than accident can erupt, which may cause release of radiations.

Water level of reactor is an important parameter in NPPs. Reactor vessel level monitoring system, measures the water level in a reactor. Specific water level is crucially important for the protection of fuel. Drop in water level exposes the nuclear fuel, which may lead to fuel

meltdown and radiation spread. This monitoring system mainly consists of sensing line and pressure transmitter. Sensing line extends from reactor vessel to pressure transmitter, which is installed outside the containment. Over a period of time Boron deposition or other impurities can cause sensing line blockage. Blockages of sensing line do not allow the accurate measurement of water level in reactor. The aim of our study is to determine the blockage in sensing line with energy of noise signal. This thesis simulates the blockages of sensing line with an equivalent pi circuit using electric-hydraulic analogy and examines the response of the system as blockage level is varied. Energy of noise signal is used to determine the occurrence of blockages. Noise signal extracted from the plant's unblocked and blocked channels and simulation model is decomposed into high frequency components and low frequency component using wavelet filter bank. The signal is decomposed up to six levels. Percentage of energy is calculated at each level for low frequency components. It is observed that percentage of energy is being reduced as blockage level in sensing the line is increased. Based on the results it is safe to postulate results of simulation model and operational data are well correlated. Variation in percentage of energy can be used as indication to determine the occurrence of blockage in sensing line.

Contents

List of Figures

List of Tables

1. Introduction

1.1 Nuclear Power

It is presumed that Nuclear power is an inexpensive source of energy. Over the last 30 years, nuclear power plants around the globe have demonstrated its capacity and capability to produce base-load at affordable prices. In addition nuclear fuel price does not fluctuate as of conventional fossil fuels. Renewable energy sources are under consideration in many countries around the world, but owing to their limited production capacity and weather dependency make their installation at limited scale and their share in energy mix policy is very low. On the other hand uranium resources are widely distributed across the globe; however fossil fuel resources are accumulated in few regions of the world. It is very likely that uranium mining will not yield tensions and crisis among nations as it has been the case for gas and oil.

These aforementioned factors strongly held belief that nuclear power is viable source of energy to meet the future demands. It is understood in nuclear industry that "Nuclear power is dangerous, if it is considered safe and it is safe, if it is considered dangerous". Continuous evaluation of the design basis and monitoring of the systems and processes in nuclear power plants are key factors to avoid any mishap. Three Mile Island, Chernobyl, Fukushima are the reminders that nuclear technology is highly unforgiving, if it is not properly monitored and maneuvered. Its effects last for the years and poses threats to the health of living beings.

1.2 Nuclear Power Plant Instrumentation and Control systems

The Nuclear Power Plant (NPP) Instrumentation and control (I&C) system, is termed as the nervous system of nuclear power plant. I&C systems senses plant physical variables e.g. water level, temperature, pressure, neutron flux, power, power-density and other variables, monitors performance of the plant and if any physical variable crosses its limits, I&C systems will shutdown the reactor to remain on safe side. I&C systems make automatic adjustments to plant operations. It also responds to failures and off-normal events and processes to ensure the safety of a plant by initiating the safety systems.

Thousand of electro-mechanical devices e.g. pumps, motors or valves are installed in NPPs, and they need to be operated in fully coordinated manner to avoid the deviations and to ensure smooth operation of the plant. The coordination among the equipments is achieved through I&C systems.I&C systems sense thousands of process variables, calculates deviations, issue commands for actuation of devices and provides information to operators. One of the important parameter to be monitored in nuclear power plant is the reactor water level. For safe transportation of heat from reactor vessel to turbine, water level of the reactor vessel is continuously monitored. Level of the reactor is vital parameter; there is strong possibility for fuel meltdown if level goes down and fuel remain uncovered for a long time in accident conditions.

1.3 Reactor vessel level monitoring system

Water Level in a reactor is measured with hydrostatic head pressure, developed by water column, in a reactor. Head pressure varies as water column level changes. Pressure transmitters, coupled with sensing lines, are used to sense the changes in water head pressure.

Variation in water level corresponds to changes in hydrostatic head pressure. Water level indication is provided to operator in Main Control Room (MCR). Reactor vessel is installed in the containment, which is highly radioactive environment. Pressure transmitter is located outside the containment to protect workers from radiations during maintenance work .Since temperature and pressure has adverse effects on the mechanical components and may damage electronics devices. This is also another reason that for installation of transmitters outside the containment. Changes in hydrostatic head are transported to pressure transmitter through hydraulic signal via sensing lines, which are extending from the reactor to pressure transmitter.

Change in hydrostatic head pressure is conveyed to the diaphragm of the transmitter through distilled water, which occupies the sensing line. Deformation in diaphragm occurs, when water pressure is impinged upon it. Deformation in diaphragm is converted into electrical signal and information is conveyed to MCR for operator information. A general layout of Reactor vessel level monitoring system is provided figure 1(Hashemian et al.[2]).Sensing lines are filled with distilled water; hydrostatic head pressure change is conveyed to diaphragm of the transmitter through water.

1.4 Blockages in Sensing Lines

In a reactor Boron is used to maintain the flux, however boron deposition is one of the main contributors of sensing line blockage. Blockages may also occur from sludge, impurities in fluid or from improper seating of the valves. Blockages in sensing lines adversely affect the measurement of water level leading to erroneous indication in the Main Control Room. These reading can mislead or confuse the operator, which may result in improper/mistaken action.

Hashemian et al.[3]indentified almost 551 events of sensing lines problems from 40,000 Licensee event reports (LER).
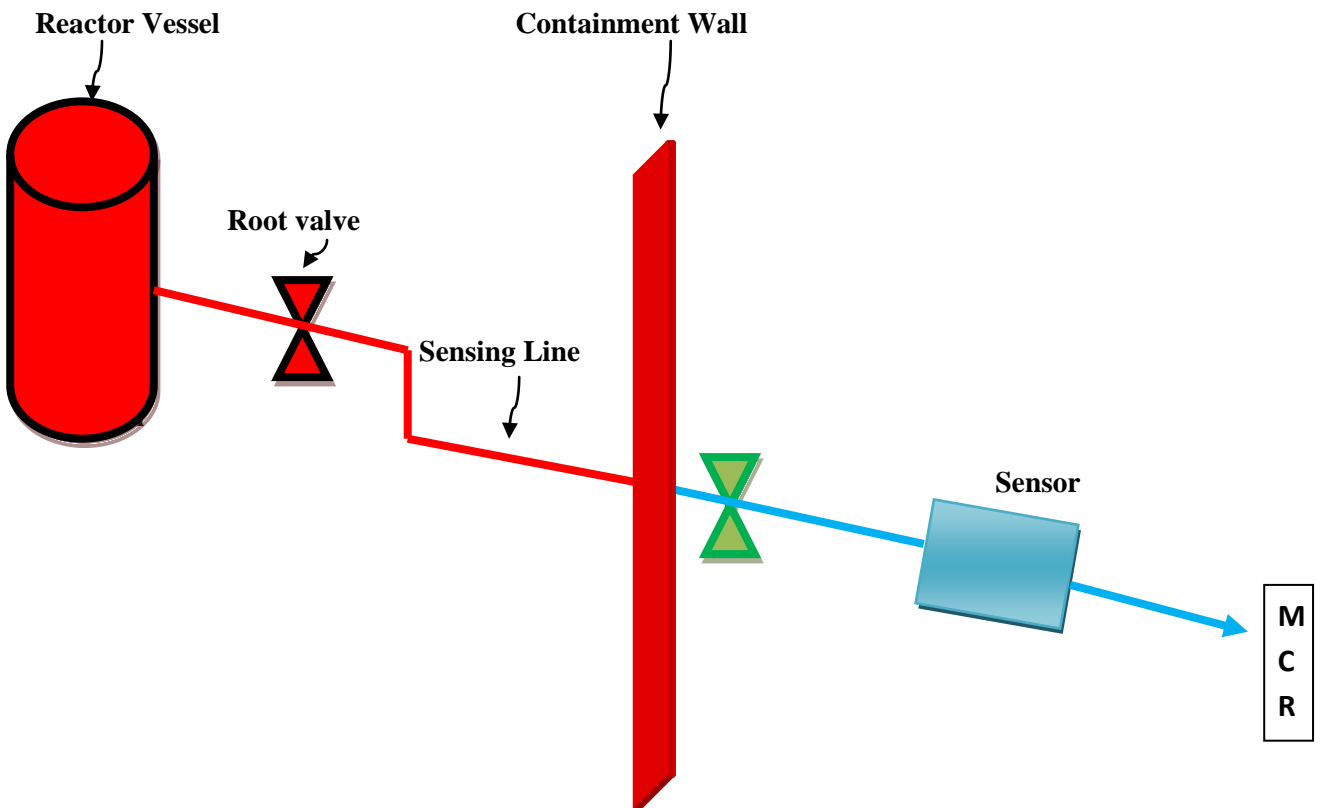
Figure 1: General layout of Reactor Vessel Level monitoring system

1.6 Problem statement

It is highly crucial for vessel level sensing system to provide accurate information to operator for taking pre-emptive actions to avoid accidents, or provision of information in case of accidents itself. Blockages may hamper the provision of accurate information to operator in control room. This research will study the impact of the blockages on system response and determine diagnostic indicator to determine the blockage level.

1.5 Research carried out

Modeling of Level sensing system using L, Tee, pi and equivalent Pi model of the transmission line is carried out. The stability of models is checked and suitable model is chosen for the analysis. The selected model is used to simulate different blockage levels and to study the response of the system. Reponses are verified by examining the operational data from the nuclear power plant.

1.6 Thesis overview

This thesis contains six chapters. Chapter 2 summarizes the literature review and techniques applied upon the problems. Chapter 3 describes the methodology. This Chapter illustrates the development simulation model, system modeling, stability of model, response of the simulation model to different blockage level and decomposition of the noise signals (operational data and simulation model) with wavelet filter bank. Chapter 4 examines the energy distribution of noise signals and provides the results of the research and chapter 5 discusses the results, documents the conclusion and provides the directions for future research. Appendix provides the details about the Haar and Daubechies wavelet transforms. The eight coefficients of unblocked noise signal are used to demonstrate the working the wavelet filter banks with Haar and Daubechies transforms.

2. Background

2.1 Literature Review

Blockages in sensing lines adversely affect the measurement of water level leading to erroneous indication in the Main Control Room. These reading can mislead or confuse the operator, which may result in improper/mistaken action.Hashemian et al.[2], identified almost 551 events of sensing lines problems from 40,000 Licensee event reports (LER). Given the importance of the level indication of the reactor, it is pertinent to establish an online monitoring for sensing lines. Hashemian et al [2] calculated the Power Spectral Density (PSD) of noise signal while assuming it to be stationary and white. The study used the PSD to determine the response time of the sensor. However plant experiments reveal that the signal is non-stationary. Figure 40 shows the periodogram of blocked and unblocked channel noise signals. It is evident that noise signals are composed of many frequencies. Thus in our opinion PSD based assessment can not reveal the true response time of the pressure sensor.

Other problem being faced is creation of voids in sensing line .Voids can be trapped into the sensing lines causing the hindrance in the measurement of levels. The resonant peak frequency deviations and peak frequency intervals are used as possible indicators for the void diagnosis Hashemian et al.[2].Operational data received from the fossil fuel power plant shows good consistency between the simulated data and field data (K.Lin et al[3]).

Hashemian et al.[4], used noise analysis technique to detect response time problems by separating the DC and AC (Noise) signal. Commercial signal conditioning equipment is used to remove the noise from the signal; noise signal is qualified by software based qualification

algorithms to check the stationarity, linearity and other parameters. Noise signal is analyzed in either frequency domain or time domain. Signal conditioning equipment and software used for the data qualification must be qualified for nuclear application and can cost the extra budget to plant owner. Vibration analysis is another technique employed to detect the blockages in circular pipes (Lile et al[6]). This is non-destructive testing. Accelerometers are installed on the circular pipe, and water flow is obstructed in pipelines using different blockage levels. Variation in flow pattern is detected using the software named Solid Works flow simulation. As variation in blockage levels developed different vibration intensities in pipes accordingly i.e. more blockages caused more vibration. Correlation is developed between the vibration intensity and the blockage level, so (Lile et al.[6]) determined blockage level from the vibration intensity. Noise analysis is also employed to detect the bubbles. Shifting of the resonant peaks towards the lower frequency regions is used as the indication for the presence of the bubbles. Experiments based on laboratory shows the peaks shifts towards the lower frequency regions and their amplitude increases when bubbles appears in the sensing line (Barbero et al.[7])

Pink noise test is another technique to check the response time of the pressure transmitter. The artificial pressure noise is produced by current to pressure convertor. The noise signal is fed to the transmitter through existing lines. This technique is used in industrial plants (Jiang et al.[8]. Hilbert transform is used as non-linearity identifier. The pressure wave is applied at the transmitter input and Hilbert transform is applied at the output signal. The linearity is manifested by dispersion in frequency v/s amplitude plot. More dispersion in data is taken as the non-linearity in transmitter hence transmitter is said to be leaked.(C.Montalvo et al.[9])

Oil loss syndrome was reported in 1987 in some Rosemount transmitters. Oil is used as isolation medium between the inner and outer diaphragm. Oil loss caused the asymmetric

behavior and provided the undesired results. Such abnormal behavior is reflected in the noise signal. Sknewness in noise signal is used as the indicator for the oil-loss (Garcia-Berrocal et al.[10]).

Long distance pressurized pipe lines are damaged because of ageing and cause leaking. To detect the leakages in lines, transporting the gas, oil or water is important before it becomes catastrophic. Acoustic emission method is employed to detect the leaks in long distance pipes(D.Ozevin et al.[11])

2.2 Techniques applied upon the problem

The noise signal extracted from the output pressure transmitter installed in RVLMS is non-stationary. Fourier analysis techniques are employed on the stationary signals. Hilbert transform is employed just to ascertain the leakage syndrome into the Rosemount pressure transmitter; however its usage in detecting the blockages in sensing lines is not found in literature so far.

Wavelet Transform (WT) is used in many areas e.g. Telecommunication, astrophysics, geology, seismology video coding etc. WT is applied upon the signals which are non-stationary. As our signals are non-stationary, therefore we selected this technique for analysis. Wavelet transform is employed upon the both synthetic and experimental data in our problem to determine the health of the sensing line during plant operation. The output signal is decomposed up to level six and energy of signal is used as indicator to determine the blockage.

3. Methodology

3.1 Development of Simulation Model

Pressure transmitter and sensing lines are two major components to form the sensing line systems. For the development of simulation model both components are modeled. The hydraulic-electric analogy is used for modeling the sensing systems. Table 1(K.Lin et al.,[13]) shows the analogy between the Electrical and Hydraulic parameters e.g., Current is analogous to Fluid flow. Table 1 tabulates the hydraulic-electric analogies

Table 1: Electric-hydraulic analogy

	Parameter	Electrical	Hydraulic
1	Integrating element	Inductance	Inertance ,p=L(dq/dt)
2	Potential Variable	Voltage/Potential difference	Pressure/head(static/dynamic)
3	Proportional element	Resistance/Reactance	Head loss (Resistance), R=P/Q
4	Differentiating element	Capacitance	Fluid Capacitance = C(dp/dt)
5	Flow Variable	Current, I	Fluid flow

3.2 Sensing Line Modeling

The analogies between the Electrical and Hydraulic parameters shown in table 1 are used for modeling of the hydraulic systems as electrical circuits. Sensing line is modeled as

transmission line and pressure transmitter as a capacitor. Three different topologies of transmission line design are given figure 2 (K.Lin et al.[13],H.Sadaat[15])

(a)Simple L Representation

(b) Pi Representation

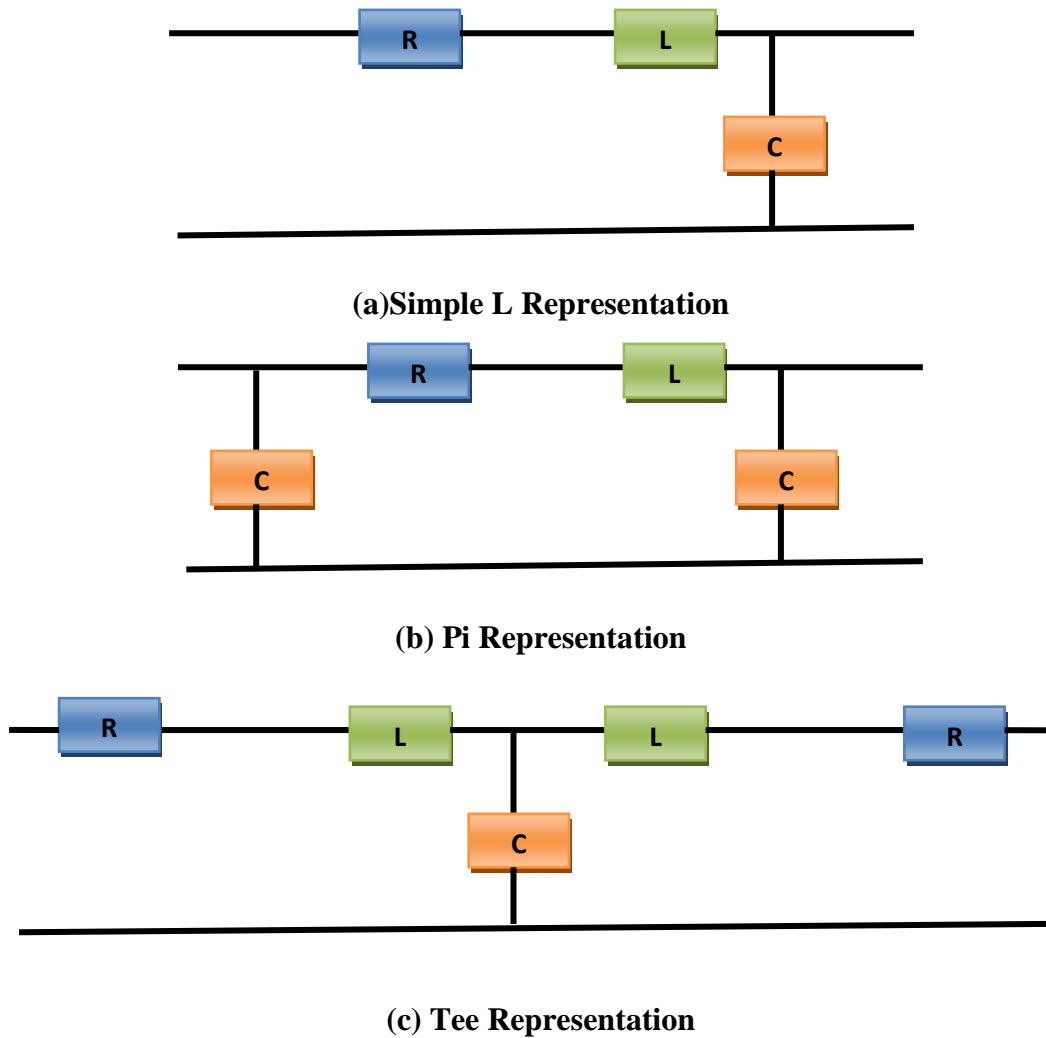**(c) Tee Representation**

Figure 2: Circuit topologies for the transmission lines

The circuit hydraulic parameters, Resistance (R), Inductance (L) and Capacitance (C) are tabulated in table 2 (K.Lin et al.[13]).

Table 2: Hydraulic Parameters

$R = \dfrac{8\mu l}{\pi r^4}$	$L = \dfrac{\rho l}{\pi r^2}$	$C = \dfrac{\pi r^2 l}{\rho c^2}$
l is length	ρ is density	l is length
μ is viscosity	l is length	r is radius
r is radius	r is radius	ρ is density
		c is speed of sound

Transfer functions are used to describe the relationship between the output and input and for analyzing the behavior of the system at different the input levels. The Transfer functions for L, Pi and Tee configurations are given.

For the L-configuration, transfer function is given by equation 1

$$H_{S(jw)} = \frac{\frac{1}{j\omega C}}{R + j\omega L + \frac{1}{j\omega C}} - - - - - - (1)$$

This is a second order under damped system with resonant frequency of

$$\omega s_o = \frac{1}{\sqrt{LC}} = \frac{1}{lc} - - - - - - - - - (2)$$

The transfer functions for the pi and tee configurations are same as given in equation (3)

$$H_{S(jw)} = \frac{1}{\left(1 - \frac{\omega^2 LC}{2}\right) + \frac{j\omega RC}{2}} - - - - - - (3)$$

Equation (3) has the resonant frequency of

$$\omega = \frac{2}{lc} - - - - - - - - - - - - - (4)$$

11

Three Transfer functions of each configuration i.e. L, Pi, Tee are plotted to select the most suitable representation for simulation model. The variables viscosity, density, length, radius given in table 3 is used according to plant configuration. Transfer function plots for the three topologies are plotted in figure 3.
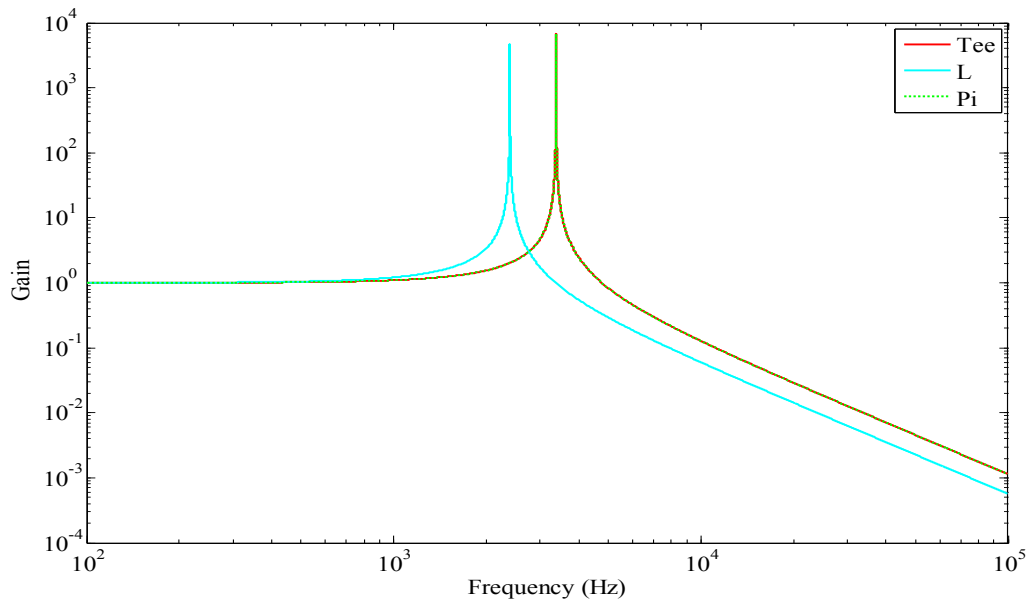
Figure 3: Transfer Function plots of L, Pi, and Tee Configuration

The Pi and tee topologies are in close approximation and can be considered more accurate than the L topology. However the drawback in Pi and Tee configurations is the appearance of single resonant peak. This peak vanishes immediately as shown in figure 3.Multiple resonant peaks are required to properly observe the behavior of system, when blockage level is increased. To overcome this problem (Matko,et al.[14]) suggested the transfer function for modeling of the pipe lines. This is named as equivalent Pi model. The transfer function of the equivalent Pi model is given in equation 5

$$H_E = \frac{1}{COSh(R+sL)sC} \text{----------(5)}$$

The resonant frequencies is derived as

$$W_n = \frac{n\pi}{2\sqrt{LC}} \text{----------(6)}$$

Where n=1,3,5,………

Equation 5 can be approximated for a second order system as [(Matko,et al.[14])

$$H_{A(S)} = \frac{1}{\left[\frac{LC}{2} + \frac{(RC)^2}{24}\right]s^2 + \frac{RC}{2} + 1} \text{--------(7)}$$

The resonant frequency is given in equation 8

$$\omega = \frac{\sqrt{2}}{LC} \text{----------------(8)}$$

The equivalent pi model is given in figure 4.This circuit used in the transmission line modeling
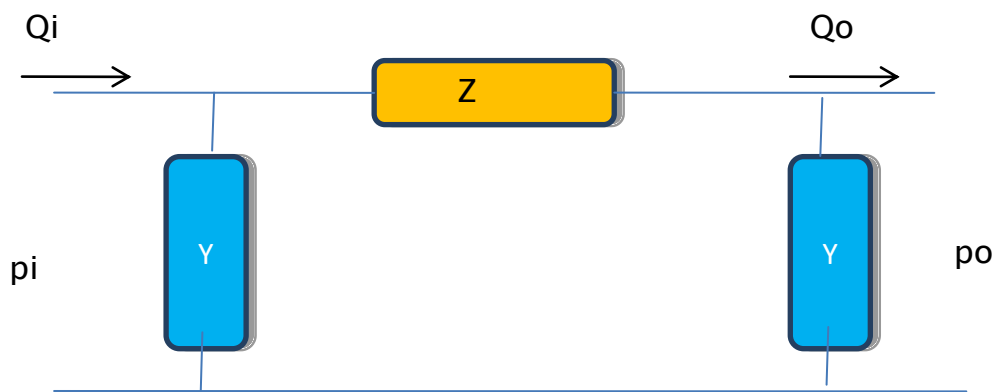

Figure 4: Equivalent Pi circuit for pressure sensing system

Pi,Po are input and output power.

Qi and Qo are input and output current.

Z is the impedance

Y is the admittance

The impedance is the opposition to current flow in a circuit, and it is the combination of ohmic resistance and reactance. Fluid flow also encounters the opposition in pipes, and this opposition is called hydraulic impedance. The hydraulic impedance for sensing lines is denoted as Z and is given in equation (9)

$$Z = Z_c \sinh\left(\sqrt{R} + \sqrt{sL}\right)\sqrt{sC} -------(9)$$

The electrical admittance is the measure of how easily current flows into the circuit and it is inverse of impedance. Since pipes are analogous to circuits and hence exhibit the admittance for fluid flow. The Hydraulic admittance is denoted by Y

$$Y = \frac{Z_c \sinh\left(\sqrt{R} + \sqrt{sL}\right)\sqrt{sC}}{\cosh\left(\sqrt{R} + \sqrt{sL}\right)\sqrt{sC} - 1} --------(10)$$

Y and Z are admittance and impedance as described in equations 9 and 10.The transfer for the equivalent pi circuit is given in equation 11

$$H = \frac{Y}{Y+Z} --------------(11)$$

The transfer function for the equivalent pi model is plotted in figure (5).Transfer function plot of equivalent pi model shows the multiple resonant frequencies as compared to L, Pi and Tee configurations.
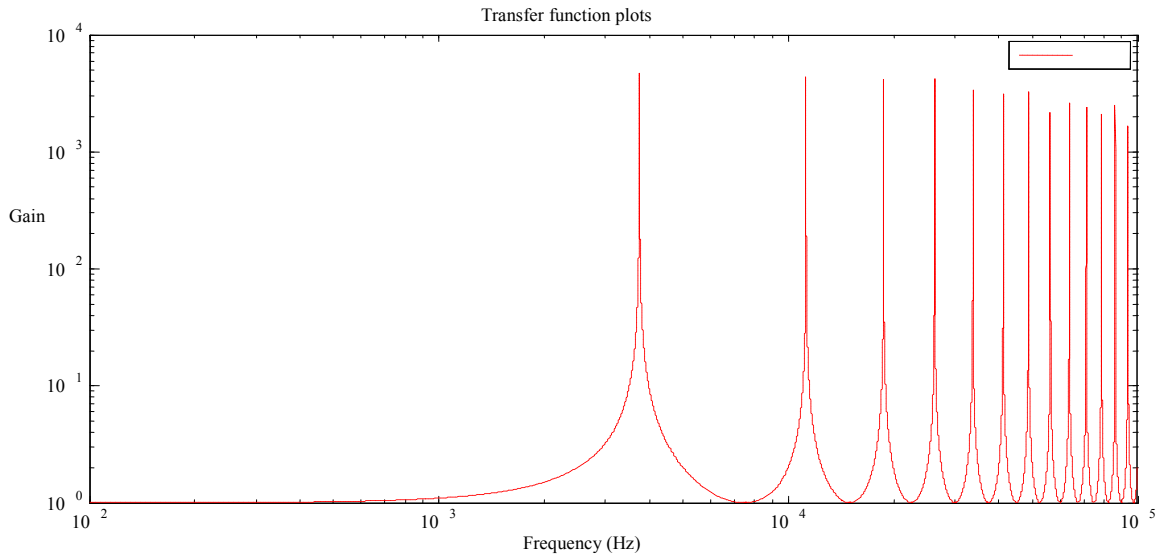
Figure 5: Transfer Function Plot of Equivalent Pi Circuit

3.3 Sensing Line and transmitter representation

The equivalent pi model is chosen after assessing different topologies for the sensing lines. Sensing Level system consists of sensing line and pressure transmitter as shown in figure 1. Therefore pressure transmitter is also modeled along with the sensing line for system analysis. Two types of transmitter are used in nuclear power plants, i.e. single diaphragm and inner structure. The single diaphragm receives the pressure from the input of the sensing lines and same is transmitted to the output circuitry. The circuit for sensing line and single diaphragm is given in figure 6 (K.Lin et al.[13]).In figure 6, Pi circuit consisting of Z and Y is the transmission line and Cd represents the transmitter. The expression for a single diaphragm is given as

$$Cd = \frac{\Delta Vd}{po} - - - - - - - - (12)$$

Δvd is the displaced diaphragm ,Po is pressure exerted upon diaphragm at time instant and Cd is the diaphragm capacity.
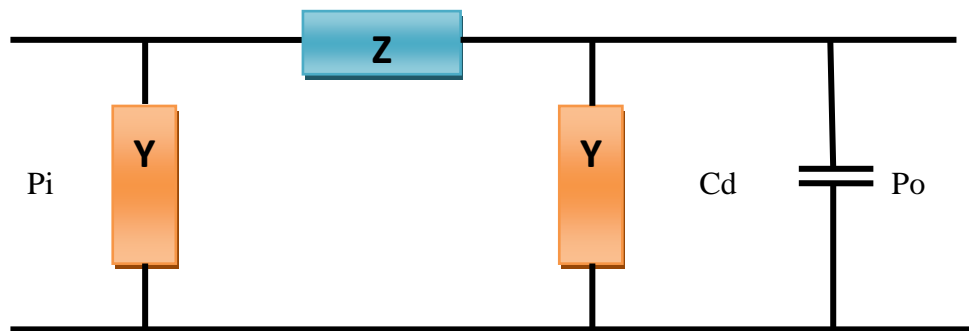
Figure 6: Pressure Sensing System with Single Diaphragm

This single diagphram configuration is proved inadequate for the laboratory experiments[Kang et al.[20]. The inner structure is used for the pressure reduction. Hydrostatic head pressure is applied at the inlet of the isolation diaphragm and is transmitted to sensing diaphragm through oil-filled channel. The model is shown in figure 7 (K.Lin et al.[13]).

Figure 7: Sensing Line with Inner Structure

Where Ci is the isolation diaphragm, Cd is the sensing diaphragm, Ri is the internal resistance. The transfer functions of both configurations are plotted in figure 8.The obvious difference between two configurations is the transfer function gain. The gain of the single diaphragm at 1Hz is almost -5 dB and for inner structure it is -35 dB. The reason is that

pressure is much more reduced at the output of the inner structure as compared to single diaphragm transmitter.

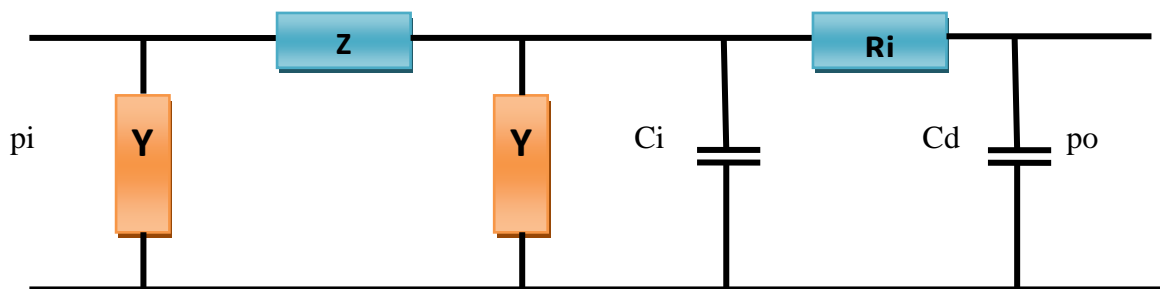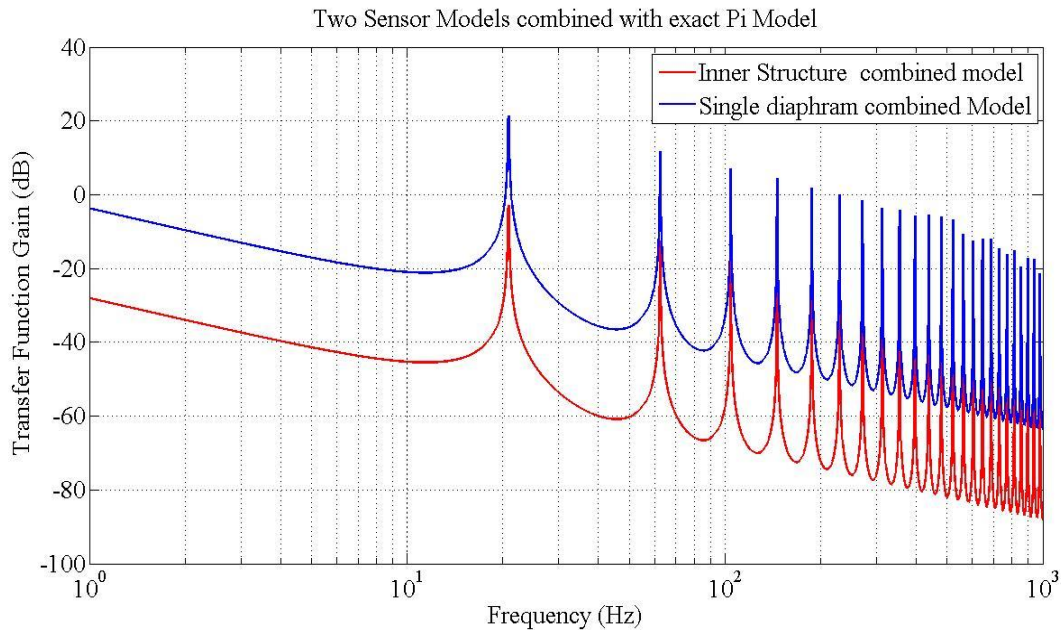**Figure 8: Inner Structure and Single Diaphragm Model for Sensing Systems**

3.4 Stability Analysis of the synthetic model

When bounded input is applied to the system, it should produce bounded output. The system response should be steady state after some time.The system must have the lesser over shoot comparing to other systems. To check the stability of the computational model of the sensing line systems ,step input is applied to models of the system as discussed in 3.1.The step response of the system is important to know the system behavior when sudden input is applied. The step response of the simple L mode is plotted in figure 9.The characteristics are calculated as well. In the same way the step response for the Pi and Tee models are plotted in figure 10.
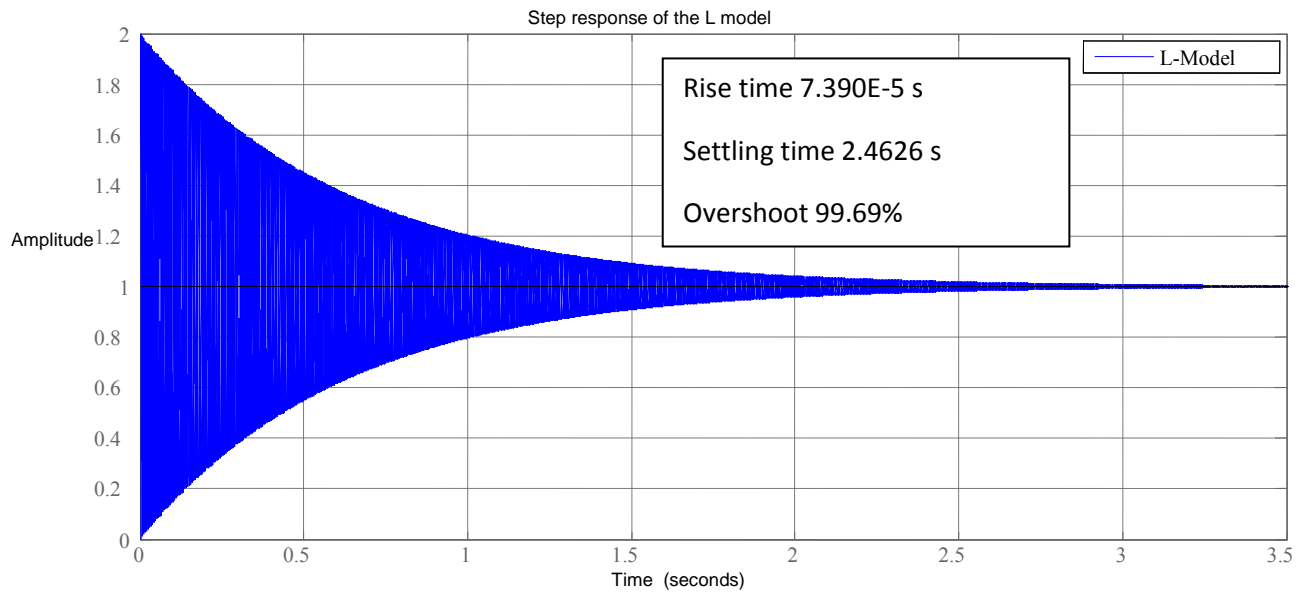
Figure 9: Step Response of the L Model
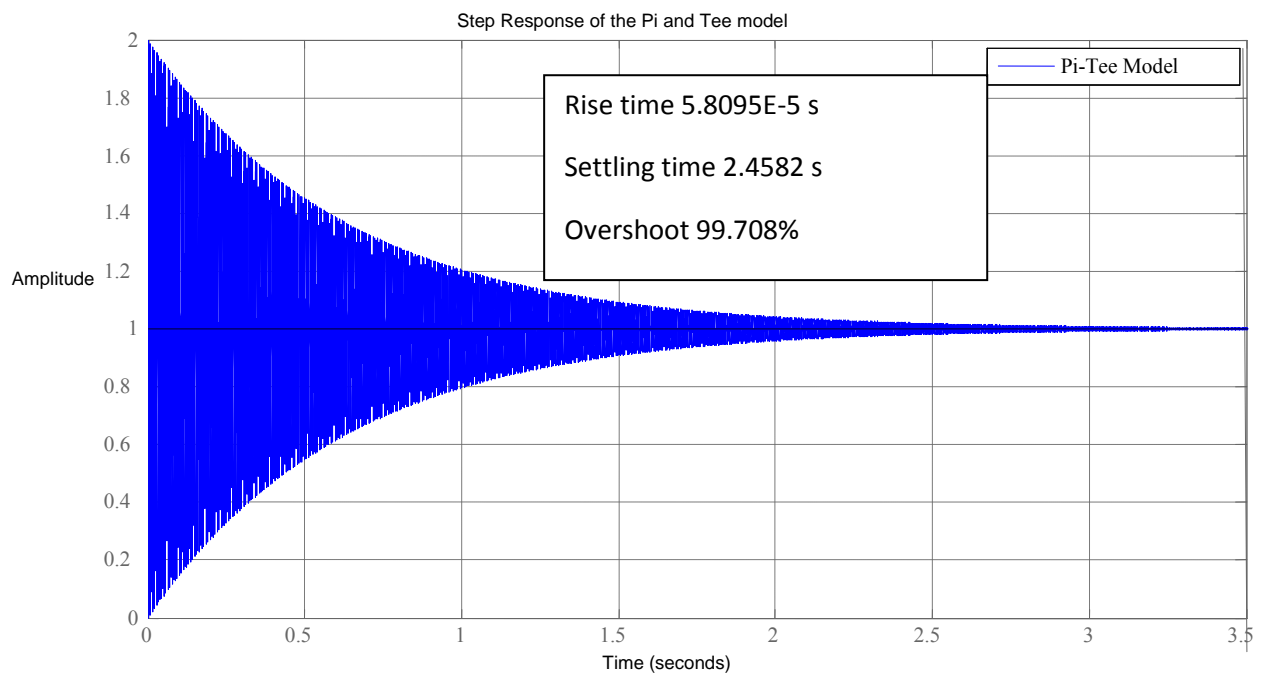
Figure 10: Step Response of the Pi and Tee Model

The equivalent pi model, which is chosen for the analysis shows good behavior as compared to L,Pi and Tee models.
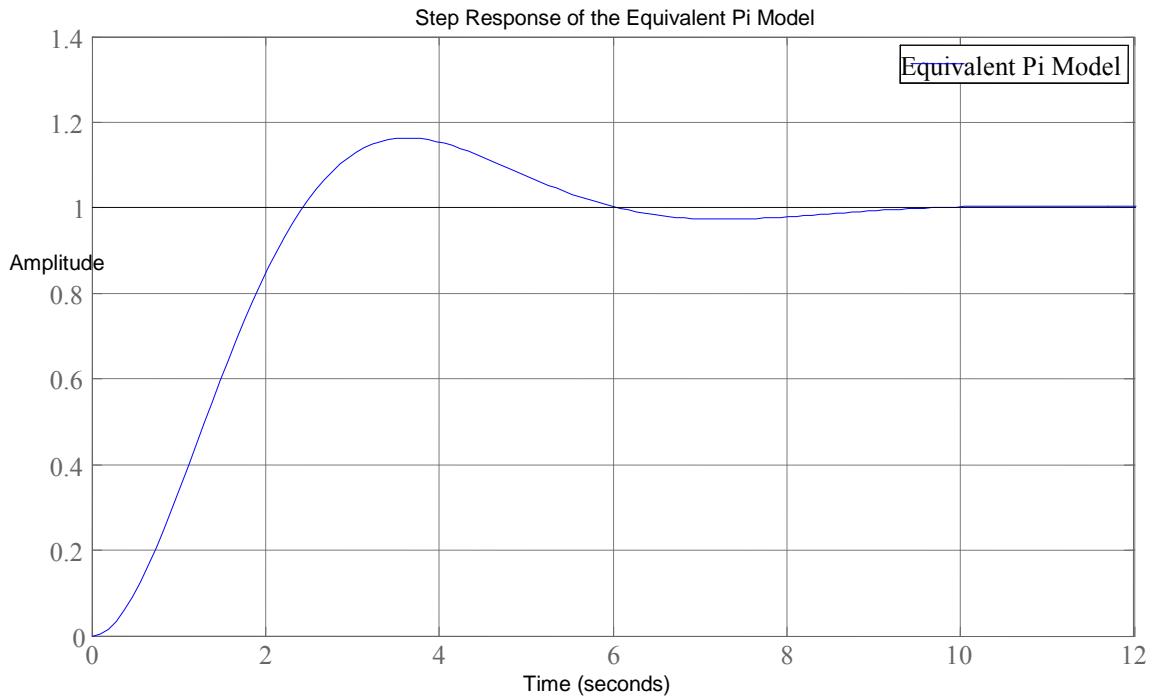
Figure 11: Step Response of the Equivalent Pi Model

The characteristics are calculated as

Rise Time: 1.6390 seconds

Settling Time: 8.0759 seconds

Overshoot: 16.2929

The overshoot of the equivalent Pi model is almost 84% reduced as compared to L, Pi and Tee models. Model stability is checked to observe the response for sudden pressure change. The equivalent pi model shows the more appropriateness for analysis.

3.5 Response of Simulation model to different blockage levels

The parameters given in table 2 shows, that variation in the radius, also changes the resistance, inductance and capacitance of the line. Blockage of lines is realized by the reduction in the radius and increase in the resistance. The inner structure configuration

(figure 7) is used for studying the effects of blockages. Three cases are considered for the blockages, normal, medium and severe. Effect of the blockages is shown in figure 12.
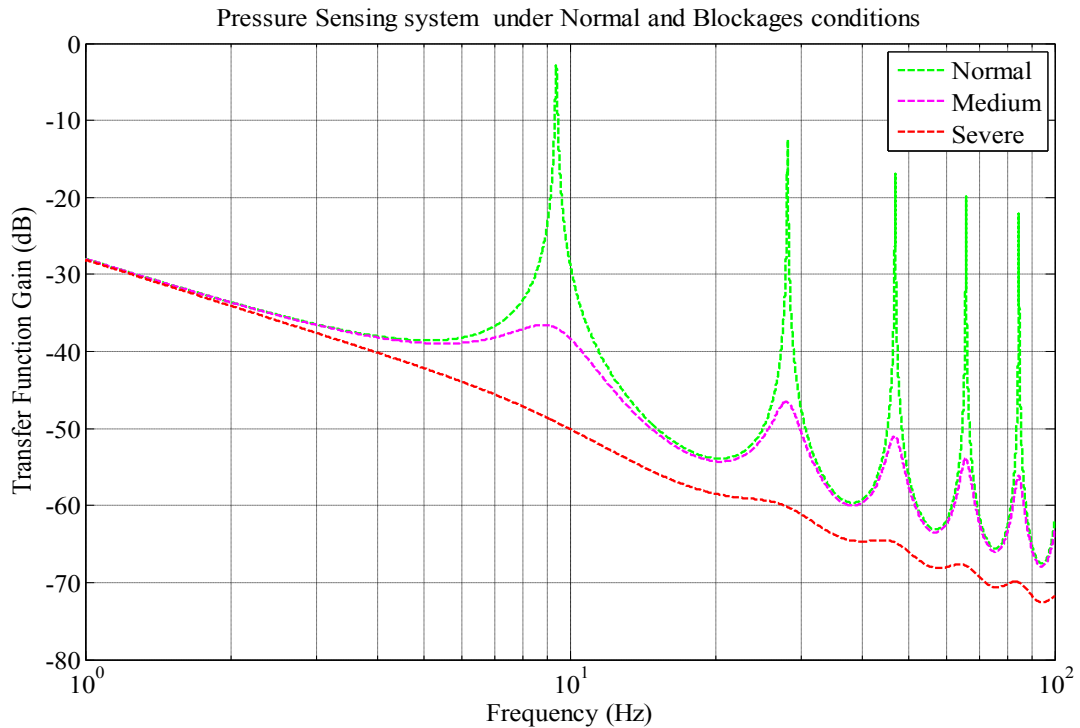
Figure 12: Pressure Sensing System under Blockages Conditions

It is observed that as blockage level is increased, the gain of the resonant peaks is also reduced. Medium and severe blockage levels have reduced gain as compared to the normal.Resonant peak gain is calculated for the three cases i.e. normal, medium and severe. Peak gain against blockage levels is given in table 3. The table 3 shows that as the blockage level is increased, the gain of the peaks is reduced e.g. for normal case the gain of the first resonant peak is -2.9534 dB and for severe blockage gain of first peak is -64.4780 dB. Another observation is that the number of peaks is also decreased. For severe blockage two peaks are not visible in the lower frequency regions, where three peaks with reduced gain are visible in higher frequency region.

Table 3: Peak Gain for Normal, Medium and Severe Blockage Level

Peak No.	Normal dB	Medium dB	Severe dB
1	-2.9534	-36.5638	-64.4780
2	-12.4979	-46.5492	-67.6143
3	-16.9476	-51.0201	-69.8808
4	-19.8648	-53.9519	Disappeared
5	-22.0628	-56.1386	Disappeared

3.6 Addition of non-stationary random noise signal to inner structure model

Non-stationary random noise is the prevalent phenomena in nuclear power plants. To match the actual scenario of the plant non-stationary random noise is added to the inner structure model as shown in 13.The noise is added to the unblocked conditions where normal radius of sensing line is used. The model depicts the scenario, which is similar to unblocked sensing line in plant. Noise is extracted for the investigation as shown in figure 14.
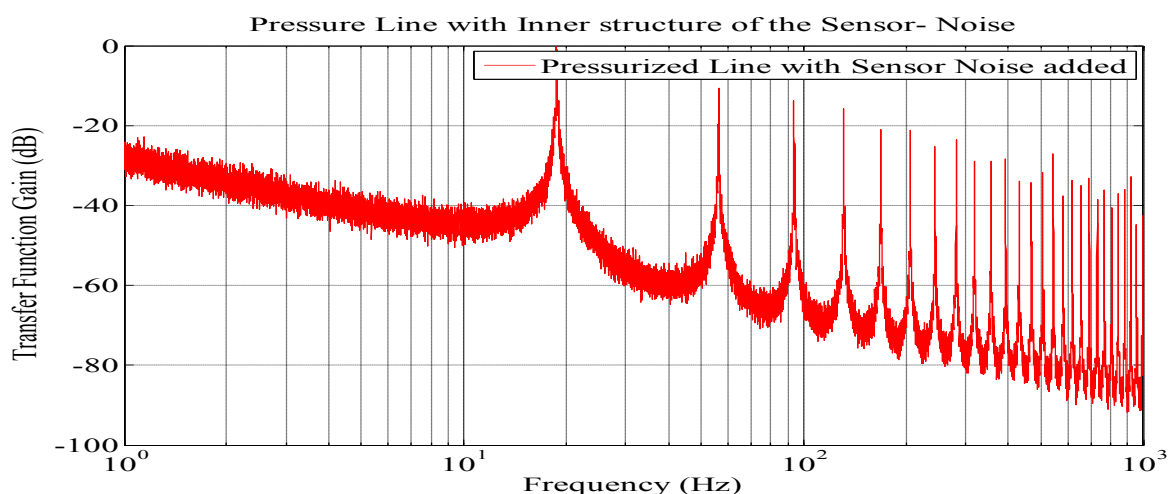
Figure 13: Noise added to the Simulation Model
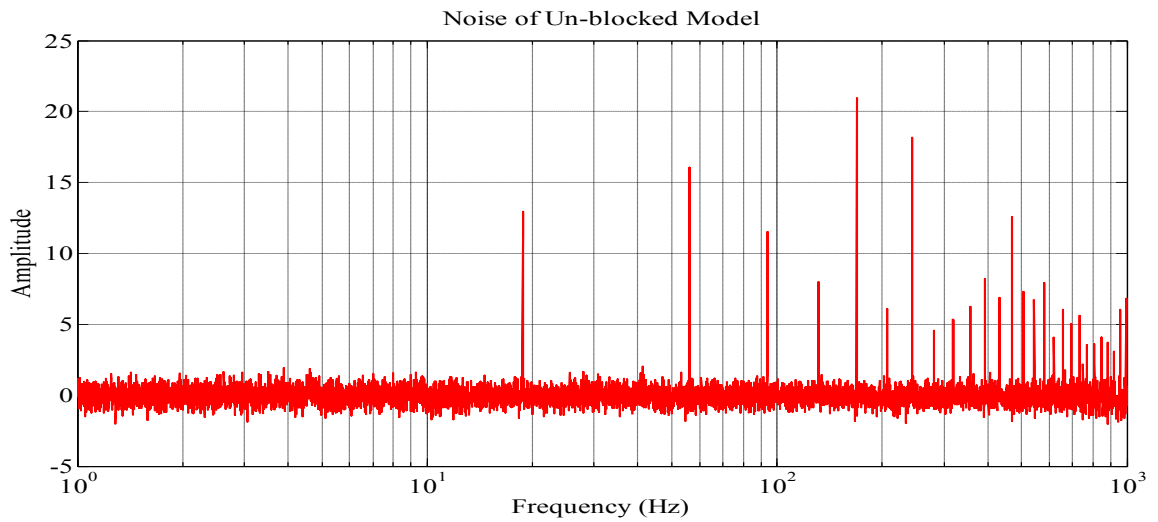
Figure 14: Noise Signal of the Unblocked Simulation Model

For the blocked condition, resistance of the inner structure model is increased to block the line and then noise signal is extracted from it. The noise signal extracted for the blocked situation is shown in figure 15
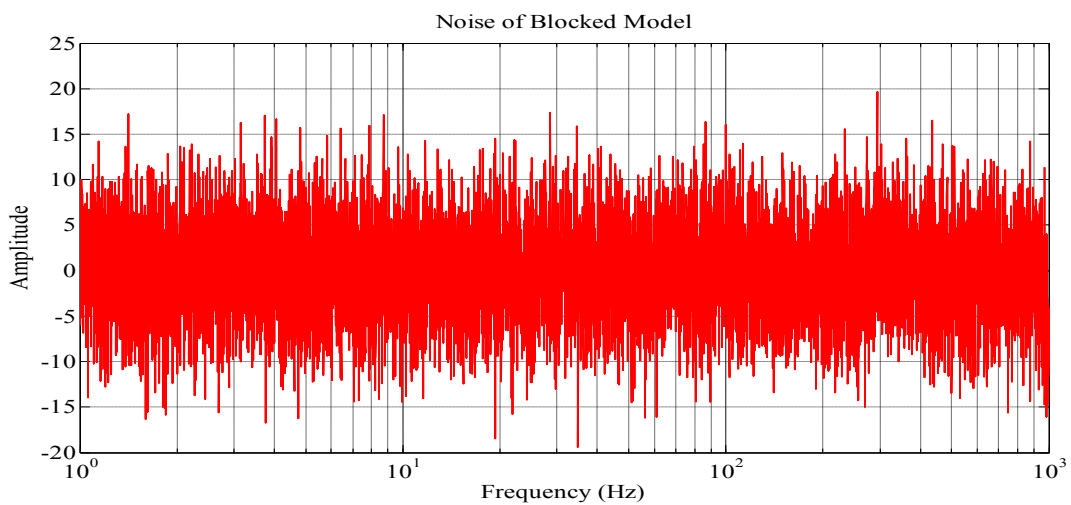
Figure 15: Noise Signal of the Blocked Simulation Model

It is clear from figure 14 and 15 that magnitude of the noise signal is increased in blocked condition of the sensing line. The noise signal is obtained from operating power plant from the output of the pressure transmitter, when sensing line is unblocked and it shown in figure

22

16.Nine thousand, six hundred and thirty one (9631) sample points are taken to adequately substantiate the analysis.
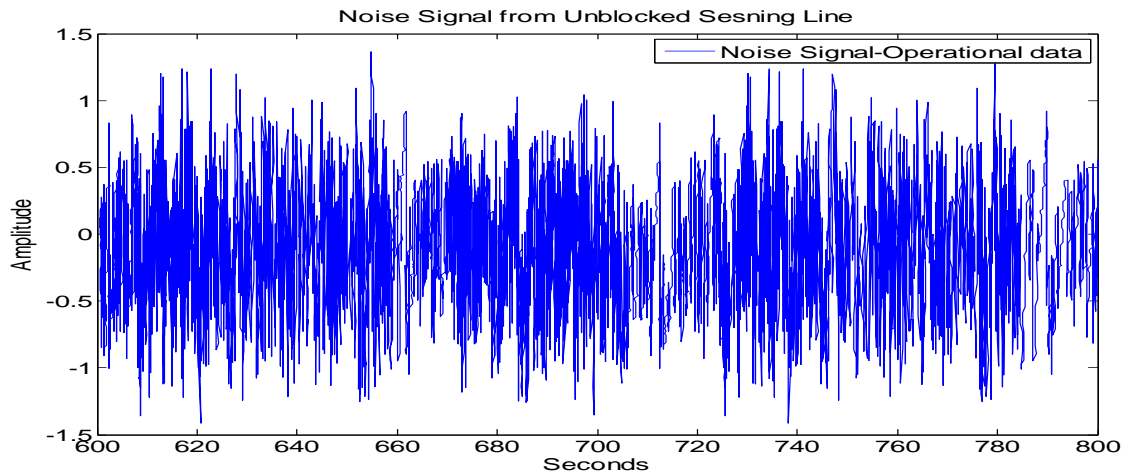
Figure 16: Noise signal of the Unblocked Sensing Line

The noise signal is also taken when the sensing line is blocked. It is shown in figure 17
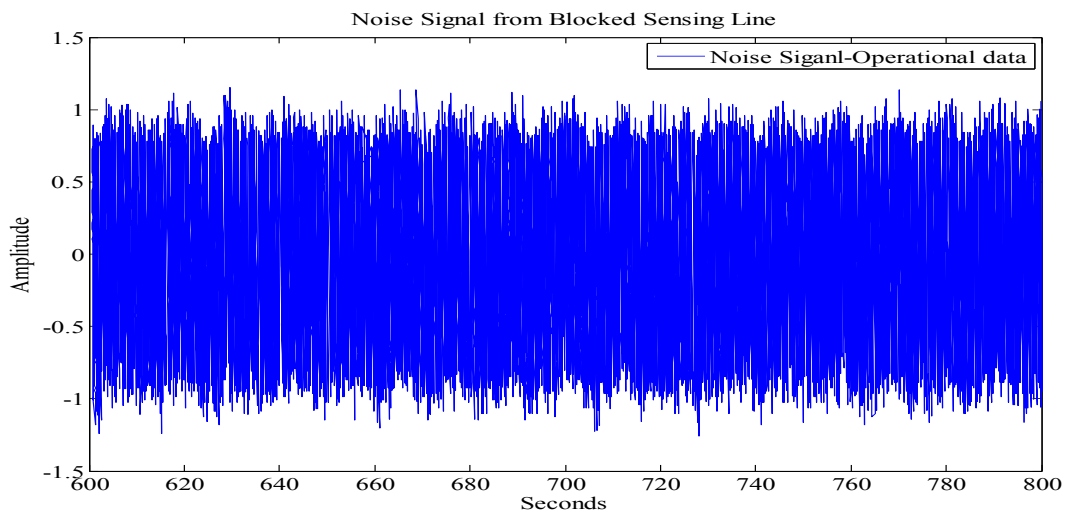
Figure 17: Noise signal of the Blocked Sensing Line

The Noise signal can be used for the online health monitoring of the sensing line. The noise is extracted from the output of the pressure transmitter then decomposed at the with wavelet filter banks to observe the changes in energy levels.

23

3.7 Overview of Transforms

Wavelet transform is an expansion of the Fourier transform. Fourier transform provides the information of the frequency content and power of the signal. However time-domain information is lost. Wavelet, transforms the signal into both time and frequency. The wavelet transform is used for the signals, which are non-stationary. Wavelet transform has the ability to decompose signal into high frequency details and low-frequency approximate signals. This technique is used for analysis of climate change to financial indices, from heart monitoring to condition monitoring of the rotating machines, and from brain activity analysis to analysis of the ECGs (Addison et al.[17]).Signal in time domain represented as series of coefficients, by comparing the signal and template function $\Psi_n^*(t)$.Equation (13) describes the relation mathematically.

$$c_n = \int_{-\infty}^{\infty} f(t)\Psi_n^*(\qquad \text{-----------} \quad (13)$$

The inner product between the two functions (t) and $\Psi_n^*(t)$ is given in equation (14)

$$\langle f, \Psi_n \rangle = \int f(t)\Psi_n^*(\qquad \text{-----------} \quad (14)$$

The inner product is the measure of degree of closeness between the signal and basis function. Inner product is basically an operation which compares the similarity between two different signals. As described already wavelet transform is used to analyze the non-stationary signals. Frequency content of the non-stationary signal varies with time. Figure 18(a) shows an example
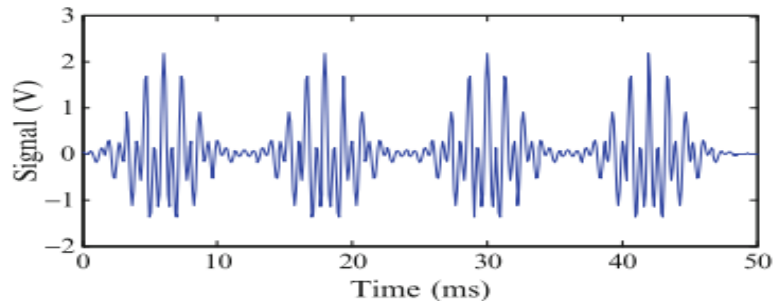
(a)
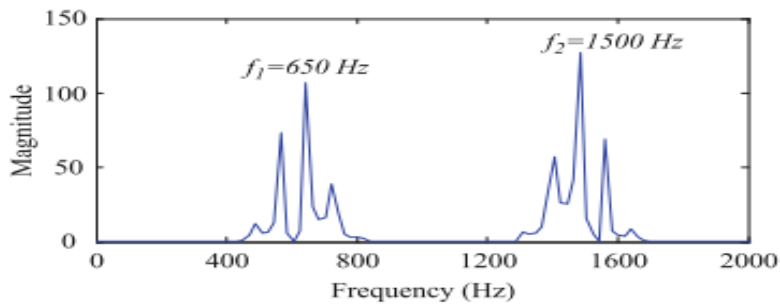
(b)

Figure 18: (a) Non-Stationary Signal, (b) Fourier transform applied on non-stationary

signals (Chia et al[43])

of non-stationary signal. The Signal is composed of two frequencies i.e. 650 and 1500 Hz, when Fourier transform is applied to the signal; it is resolved into frequency components available within the signal as two frequencies exhibited by signal which are shown in figure 18(b) i.e.650 and 1500 Hz

3.7.1 Fourier Transform

Fourier transform is a mathematical tool for decomposing signal into frequency components. Fourier transform is inner product of a signal in time domain and complex exponentials as given in equation 15,

$$X(f) = \langle x, e^{i2\pi ft} \rangle = \int_{-\infty}^{\infty} f(t) e^{-i2\pi ft}\, dt - - - - - - (15)$$

It is assumed that signal has finite energy,

$$x(t) = \int_{-\infty}^{\infty} X(f) e^{i2\pi ft}\, df - - - - - - - - (16)$$

The Fourier transform is basically the convolution between the signal in time domain f(t) and basis or template functions i.e. sine and cosine. The Fourier transform calculates the degree of closeness between time domain signal f(t) and the basis functions, and provides information of frequency components available in the signal as shown in Figure 19.The disadvantage of the Fourier transform is that temporal information is lost. Figure 18(b) illustrates that two frequency components are present in signal, but at what time these two different frequencies occur, it is not known. The occurrence of particular frequency component available in signal at particular time remains unknown. The application of the Fourier transform is limited only up to stationary signals.
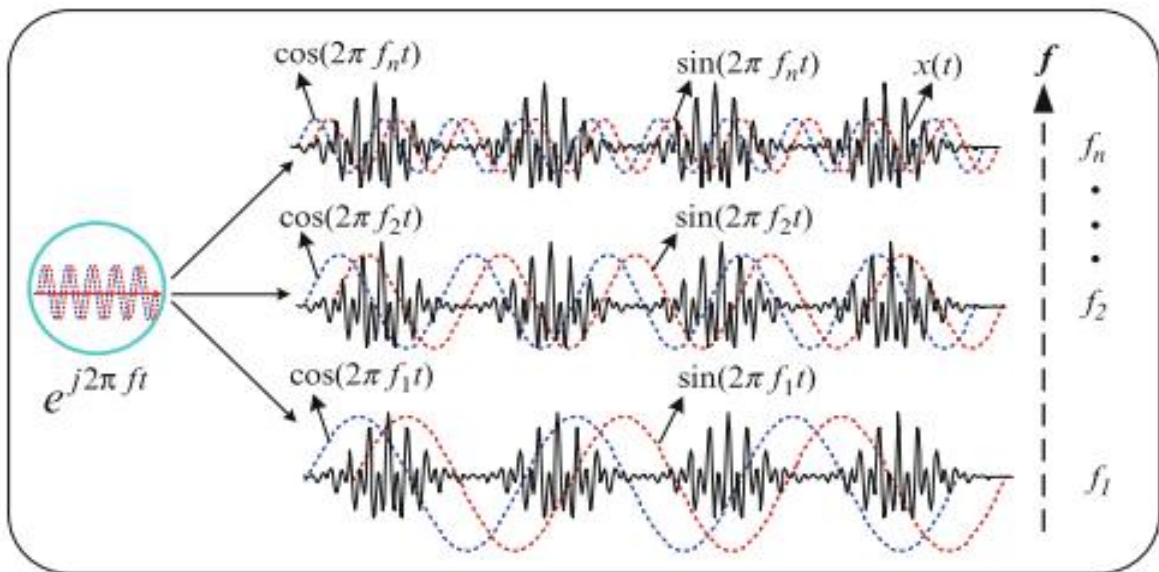
Figure 19: Illustration of Fourier transform (Chia et al.[43])

26

3.7.2 Short Time Fourier Transform (STFT)

To overcome the shortcoming of Fourier transform, a fixed window is applied to the signal and shifted on time axis to perform the time-localized Fourier transform. As shown in Figure 20, the STFT utilizes the sliding (fixed length and width) window function g(t). Time-localized Fourier transform is performed upon the signal x(t). Window is moved along the time axis. The signal appears to be stationary within the window. STFT decomposes a time domain signal x(t) into a two-dimensional time-frequency domain. The window has fixed dimensions. STFT is expressed mathematically

$$\mathbf{STFT(\tau, f)} = \langle \mathbf{x, g_{t,f}} \rangle$$
$$= \int_{-\infty}^{+\infty} \mathbf{x(t)g_{t,f}}^*\mathbf{(t)dt}$$
$$= \int_{-\infty}^{+\infty} \mathbf{x(t)g(t-\tau)e^{-i2\pi ft}dt} - (17)$$

What should be shape of window function e.g. Gaussian, Elliptic or rectangular and what should be size of window is a question to be considered**.** If window is narrow, STFT cannot provide good localization in frequency domain and if window is very wide, it is not able to give good localization in time domain.

g(t)=1 STFT will become Fourier transform, providing excellent frequency localization but no time information and g(t)= *δ(t)* STFT provides excellent time localization but no frequency information, so we can say that it is extremely difficult to increase time and frequency resolution simultaneously, if one is improved other will suffer. Precisely we can say that STFT analysis is dependent on the length of the window g(t),so either time resolution will be good or frequency resolution
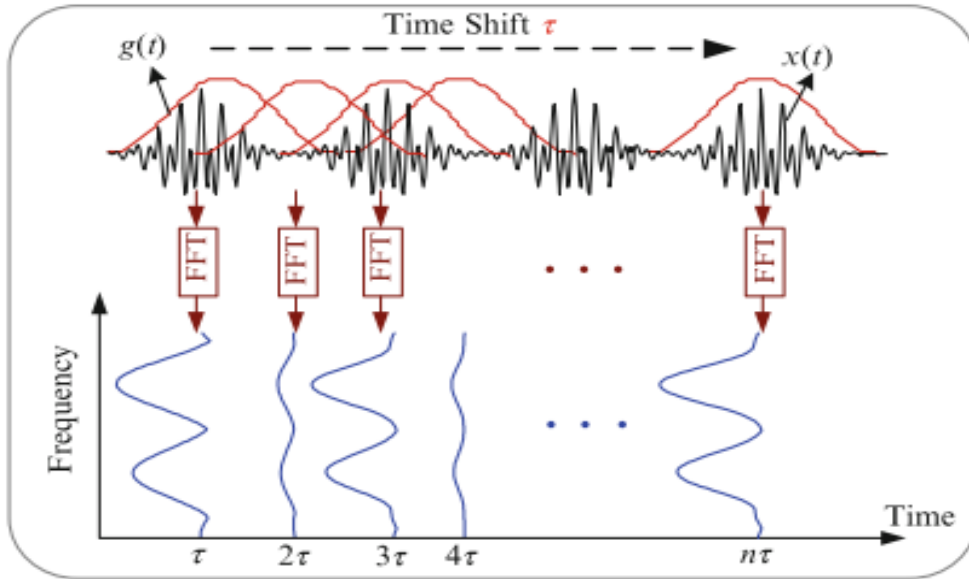
Figure 20: Illustration of Short Time Fourier Transform (Chia et al.[43]),

This phenomenon is described by the uncertainty principle, it is similar to Heisenberg uncertainty principle in quantum physics, according to this principle it is impossible to know the position and momentum of particle at the same time.

According to principle time and frequency resolutions of the STFT window cannot be chosen at the same time. The STFT window is fixed

$$\Delta\tau \cdot \Delta f \geq \frac{1}{4\pi}$$

$$\Delta\tau^2 = \frac{\int \tau^2 |g(\tau)|^2 d\tau}{\int |g(\tau)|^2 d\tau} \qquad \Delta f^2 = \frac{\int f^2 |G(f)|^2 df}{\int |G(f)|^2 df}$$

As shown in figure 21, the multiplication of the time and frequency resolutions of the fixed length window function (Δτ∗Δf=area of window) are the same regardless of the window size

(Δτ∗Δf=area of window)
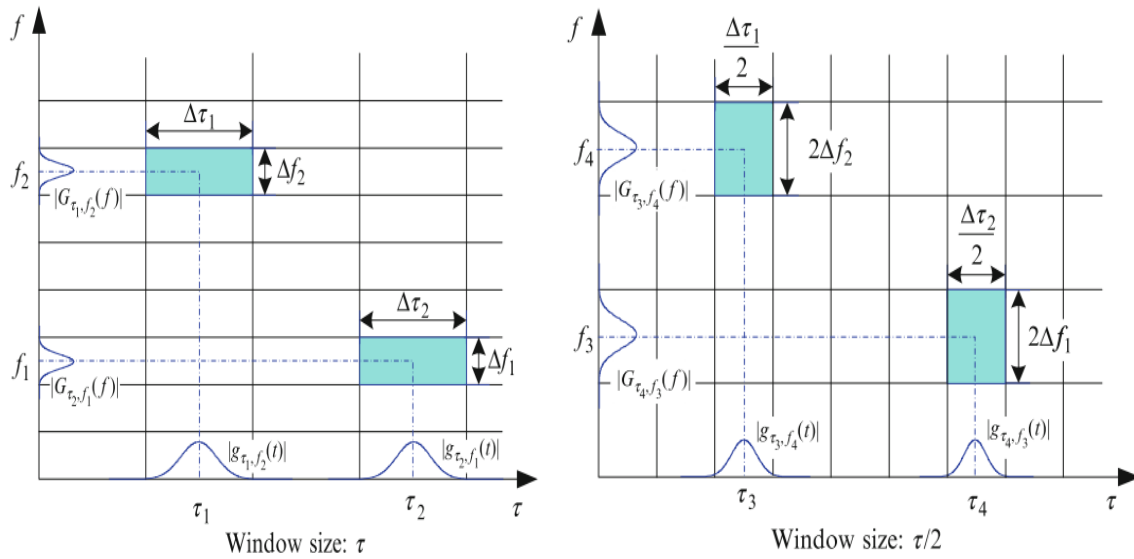
Figure 21: Illustration of the Fixed Length STFT Window Function((Chia et al.[43]),

3.7.3 Wavelet Transform

STFT cannot provide accurate time and frequency information of a signal simultaneously. Wavelet transform is developed to remove the limitations of STFT.Wavelet transform employs the variable length window functions (i.e. resolutions) for analyzing the frequency content of the signal. Wavelet transform compares the time domain signal f(t) with set of wavelet functions.

Ψ called mother wavelet or template function. Mother wavelet forms the basis of the signal by dilation and translation as shown in figure 22.

29
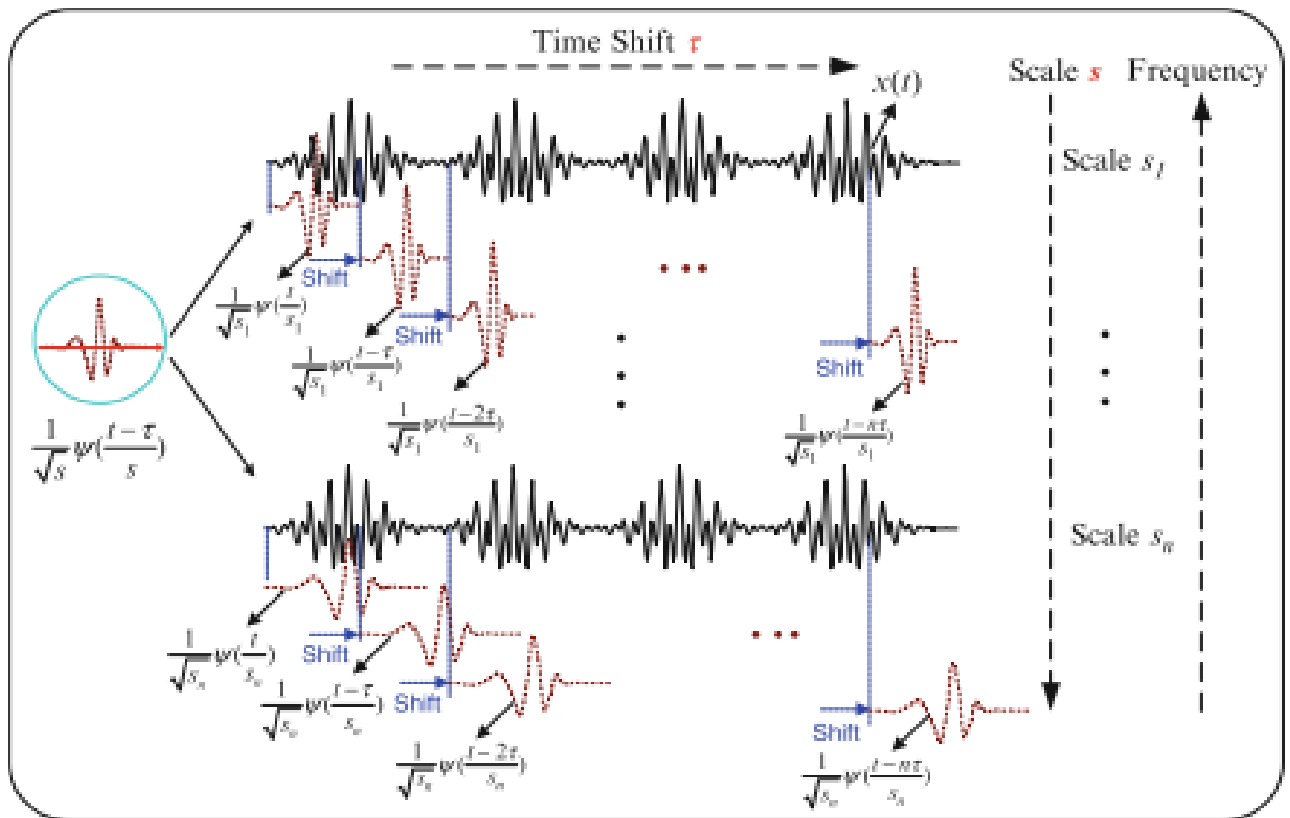
Figure 22: Illustration of the Fixed Length Operation of Wavelet Transform(Chang et al [43]

Wavelet transform is expressed mathematically by equation 18

$$wt(s.\tau) = \langle f, \Psi_{s,\tau} \rangle = \frac{1}{\sqrt{s}} \int_{-\infty}^{\infty} f(t)\Psi^*\left(\frac{t-\tau}{s}\right)dt - - - (18)$$

is translation of the wavelet that changes along the time axis and s is the dilation or scaling of the wavelet function. Changes in s not only alter the spectrum of window function, but also vary the resolution of the time-frequency window. Figure23 illustrates the variations in time and frequency resolutions of the Morlet wavelet at two different locations of the time–frequency plane, $(\tau_1, \eta/\sigma_1)$ and $(\tau2, \eta/\sigma2)$
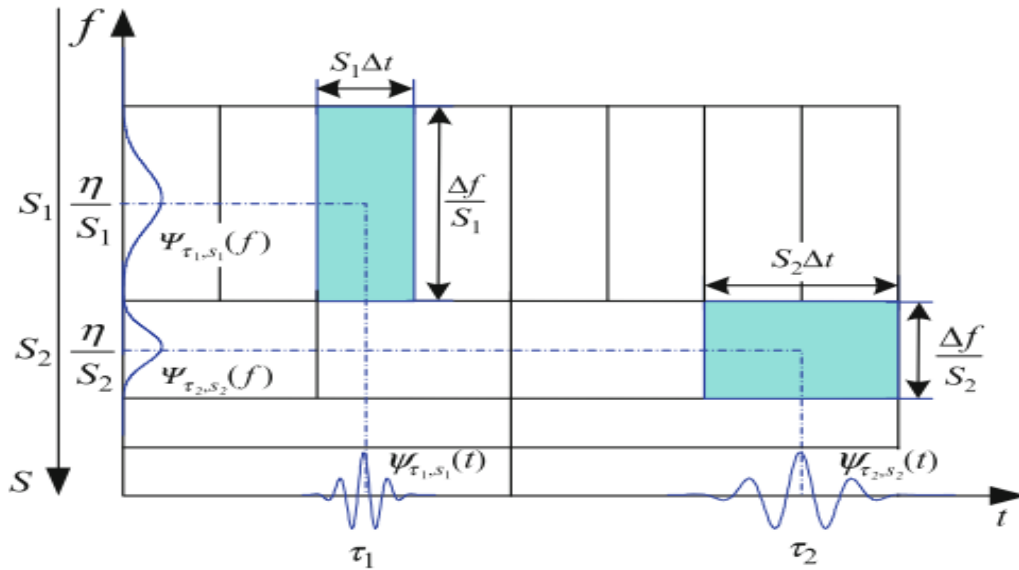
Figure 23: Illustration of Translation and Scaling of the Window Function (Gokhale [36])

With variations in scale and time shifts of the mother wavelet Ψ ,the signal is decomposed into high and low frequency components.Small scales are used for decomposing the signal into high frequency components and large scales for used for low frequency components.

3.7.4 Continuous Wavelet Transform

Continuous wavelet transform(CWT) is summation of the all scaled and shifted versions of wavelet transform i.e. mother wavelet It is expressed mathematically as given in equation 19

$$f(a,b) = \frac{1}{\sqrt{b}} \int_{-\infty}^{\infty} x(t)\Psi\left(\frac{t-a}{b}\right) dt ------(19)$$

The time shifting is realized by changing translation parameter a,and scaling is done by changing parameter b.Translation parameter is proportional to time and specifies the location of the mother wavelet in time.The scaling parameter b is inversely proportional to frequency.The change in b not only varies the frequency of the wavelet but its resolution as well.By choosing the larger values of scaling parameter b,lower frequencies of the signal are

31

extracted and with smaller values of scaling parameter b higher frequencies are extracted. The energy remains constant as it is normalized with   .If the continuous wavelet transform of g(t) is G(s,τ) and of f(t) is F(s,τ), then the continuous wavelet transform of z(t) = K₁g(t) + K₂f(t) is described as

$$Z(s, \tau) = K_1 G(s, \tau) + K_2 F(s, \tau) - - - - - - - (20)$$

Equation 20 is the superposition property .An other important point of CWT is **covariance** under shifting and scaling.If continuous wavelet transform of f(t) is F(s,τ),   then the transform of F(t-t₀) is

$$F(s, \tau - t_0) - - - - - - - (21)$$

This implies that coefficients of F(t-t₀) is obtained by shifting the wavelet coefficients of f(t) along the time with t₀.if continuous wavelet transform of F(t) is F(s,τ), then the CWT of x(t/a) can be described as

$$\sqrt{a} X \left(\frac{s}{a}, \frac{\tau}{a} \right) - - - - - (22)$$

It means that when signal is shifted by translation parameter a, its corresponding wavelet coefficients are also shifted by translation parameter along the scale and time axes. The translation parameter slide the mother wavelet along the time axis and scaling parameter vary the size of the mother wavelet, so all the windows used for the signal analysis are the scaled and dilated versions of the mother wavelet. As shown in figure 22, the mother wavelet is placed at time=0 and it slides along the time scale by changing the value of the translation parameter. Mother wavelet is multiplied with corresponding signal and integration is done all over the times. Scaling the wavelet function changes its size, lower scales decomposes the signal into higher frequency components and higher scales decomposes the signals into lower frequency components.

3.7.5 Discrete Wavelet Transform

Signal acquired with experiments are not continuous on time axis but are sampled at discrete time intervals. In CWT we observed that time-frequency resolution is performed by shifting and scaling of the mother wavelet. It is discovered that such analysis is performed using multi-resolution filter banks as given in figure 28.

Discrete signal is applied at the input of the filter bank and it is down sampled by ½ to produce the sub-band of signals. This process is called the analysis and if signal is reconstructed from the sub-band signals by up sampling this is called the synthesis .As we are concerned with the analysis of the signal .Figure 28 is analysis filter banks.

The filter banks decompose the signal into frequency bands. Discrete time signal is passed through the filters banks g[n] that is low pass filter and h [n], which high pass filter. High pass and low pass filter separates the high frequency and low frequency components of x[n].The high frequency components are referred to as details and low frequency components as approximations. Details and approximations contain the half frequency samples of the original signal. In other words we can say that when high and low frequency components are combined, original signal is obtained for the corresponding level. Figure 25 illustrates the operation of the decomposition of the signal. The signal is applied at the input of the filter bank,and it is decomposed into sub-band signals by the wavelet function The narrow scale decomposes the signal into high frequency components and higher scale into low frequency components. This combination of the high pass and low pass filter is called quadrature conjugate filter(QCF) Figure 24 illustrates the one level decomposition of the signal into low and high frequency components. The relationship between the wavelets and filter banks that implement the transform is given by the

$$\phi(t) = \sqrt{2} \sum h[k]\phi(2t-k) \ ----------- (23)$$

Where $\phi(t)$ is the scaling function, which determined by applying filter coefficients recursively, since multi-resolution convolves the input vector after shifting and scaling. The equation 23 is explained as follows,

The scaling coefficients of Daubeches 4(Daub4) is given by

$$h1 = \frac{1+\sqrt{3}}{4\sqrt{2}}, h2 = \frac{3+\sqrt{3}}{4\sqrt{2}}, h3 = \frac{3-\sqrt{3}}{4\sqrt{2}}, h4 = \frac{1-\sqrt{3}}{4\sqrt{2}},$$

One level decomposition of the signal with Daub 4 is achieved as

$$\Phi_1^1 = (h1, h2, h3, h4, 0, 0, 0, 0 \ldots 0)$$

$$\Phi_2^1 = (0, 0, h1, h2, h3, h4, 0, 0, \ldots 0)$$

$$\Phi_3^1 = (0, 0, 0, 0, h1, h2, h3, h, 0, 0, 0, 0 \ldots 0)$$

This process is recursive. The important point is that Φ_2^1 is translation by two time units of the first signal Φ_1^1 and Φ_3^1 is translation of four time units of first signal.

$\psi(t)$ is the wavelet function and it is given by equation 24

$$\psi(t) = \sqrt{2} \sum g[k]\phi(2t-k) \ ----------- (24)$$

It is explained as follows, The wavelt number of Daub 4 are defined as

$$g1 = \frac{1-\sqrt{3}}{4\sqrt{2}}, g2 = \frac{\sqrt{3}-3}{4\sqrt{2}}, g3 = \frac{3+\sqrt{3}}{4\sqrt{2}}, g4 = \frac{1+\sqrt{3}}{4\sqrt{2}}$$

One level decomposition of signal with wavelet function is same as scaling function i.e.

$$\psi_1^1 = (g1, g2, g3, g4, 0, 0, 0, 0 \ldots 0)$$

$$\psi_2^1 = (0, 0, g1, g2, g3, g4, 0, 0, \ldots 0)$$

$$\psi_3^1 = (0, 0, 0, 0, g1, g2, g3, g, 0, 0, 0, 0 \ldots 0)$$

This process is also recursive

$h[k] \ and \ g[k]$ are pair of quadrature conjugate filter mirror filters (low- pass and high pass

filters) which are related by

$$\mathbf{g_k} = (-\mathbf{1})^k \mathbf{h}_{-(k-1)} ------- (25)$$

Where k is integer
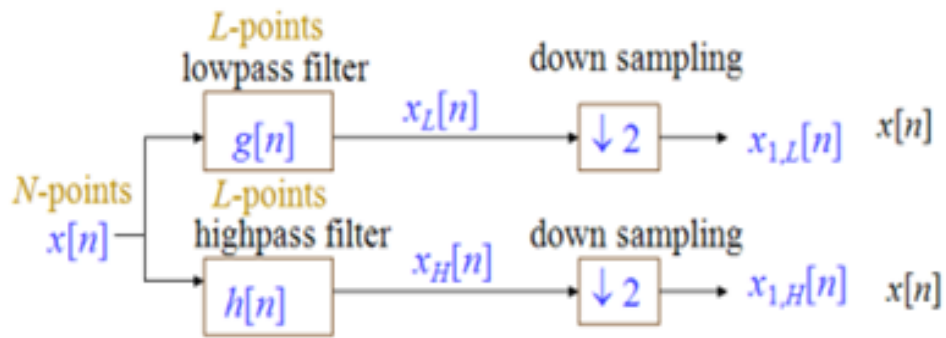
Figure 24: One level Filter banks for decomposition of the signal(Gokhale [36])

Note: *H* - Low pass filter; *G* - High pass filter; *A* - Approximate information; *D* - Detailed information
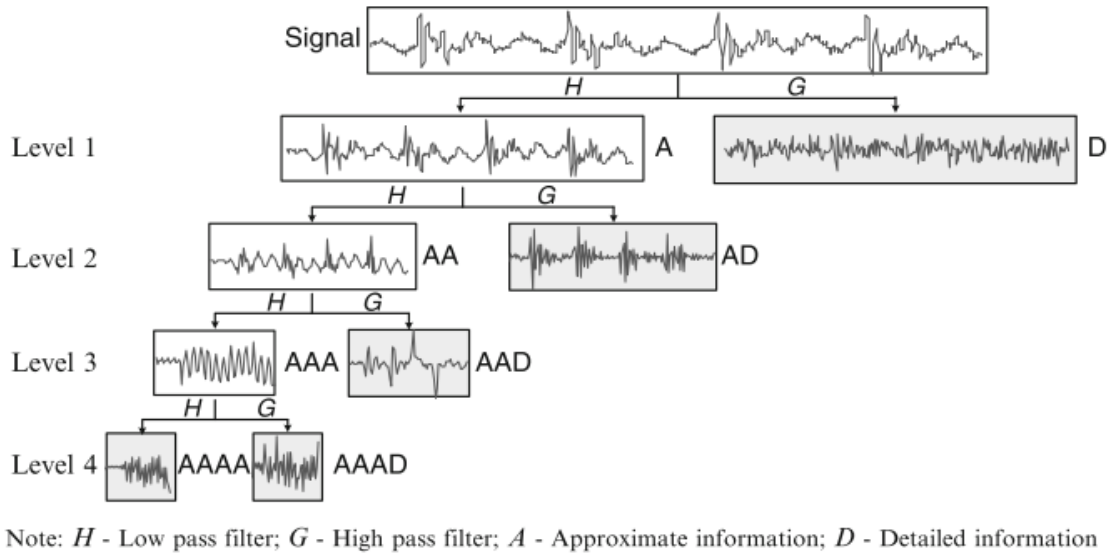
Figure 25: Decomposition of the Signal inHigh & Low frequency components (Gokhale

[36])

Commonly used wavelets for the DWT are decribed brefiely as follows:

Haar Wavelet, is orthogonal and symmetric,exhibits linear phase characteristics.The Linear phase assures that when a wavelet filtering is conductedupon a signal, no phase distortion occurs in the filtered signal. This wavelet isthe simplest ,with the highest time resolution.it is given as follows

$$\Psi(t) = \begin{cases} 1 & 0 \le t < 0.5 \\ -1 & 0.5 \le t < 1 \\ 0 & \text{otherwise} \end{cases} \tag{26}$$

The rectangular shape of the Haar wavelet leads to a low frequency resolution.
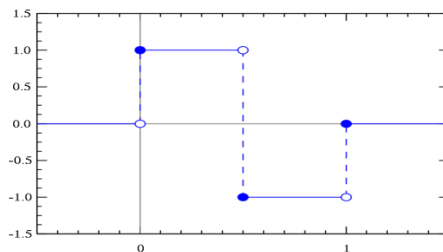
Figure 26: Haar Wavelet (Gokhale [36])

Another base wavelet is Daubechies, it is orthogonal,asymmetric and introduces a large phase distortion, when applied on the singal. The wavelet can not be used for the operation,where linear phase is requried for the output signals. Daubechies 2 and 4 transforms are givenin Figure 27.
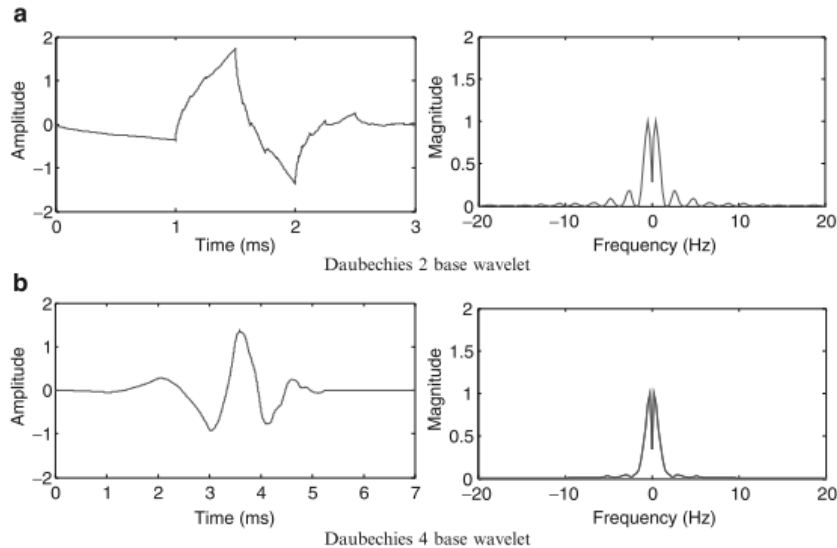
Figure 27: Daubechies Wavelets of Base 2 and 4 (Gokhale [36])

These wavelets are commonly used for the investigation of fault diagnosis of bearings and automatic gears.There are also other wavelets which are basically extension of the Daubechies i.e.**Coiflet** and **Symlet**.Daubechies has compact support for noise removal and decomposition of the signal

3.7.6 Selection Criteria for base Wavelet

Two approches are used to examine the performacne of the basewavelets,one is qualitative and other is quantitative.Three characteristics i.e.orthogonality,symmetry and compact support are generally used as the parameters for the selection of the base or mother wavelet.The orthogonality describes that,inner product of the wavelet yields unity with itself and product is zero with scaled and shifted versions of the base wavelets.This property is suitable for the decomposition of the signal into un-overlapping frequency components.

Mother wavelet serves as the linear phase filter when they are symmetric.Another approach is shape mathcing that is qualitative.Shape matching is generally not used for the analysis, as it is difficult to match the shape with just visual comparison. This disadvantage calls for quantitative measures for the selection of base wavelet selection. Two more quantitative creteria are used to select optimal wavelet base, i.e. maximum energy and minimum Shannon entropy.

The energy content of a signal f(t) is calculated by

$$E = \int |x(t)|^2 dt ------(27)$$

$$E = \int |f(t)|^2 dt ----------- (28)$$

It is also calculated from its wavelet coefficients

$$E = \int \int |ft(s, \tau)|^2 ds d\tau --------(29)$$

The above equation can be written as

$$E(s) = \int |wt(s, \tau)|^2 d\tau -------(30)$$

If the major frequency component that resides into specific scaling level,then wavelet coefficients will have relatively high magnitude at that level.The energy related to that component is extracted from the signal,by applying suitable wavelet transform. Therefore, base wavelet having capability to extract the largest amount of energy from the signal is desired.

The **entropy** referred here is the entropy of the wavelet coefficients, instead of the signal itself. The energy distribution of the wavelet coefficients is given by Shannon entropy.

$$E_{\text{entropy}}(s) = -\sum_{i=1}^{N} p_i \cdot \log_2 p_i$$

p_i is the energy probability distribution of wavelet coefficients and is mathetically described as in equation 30

$$p_i = \frac{|wt(s,i)|^2}{E_{\text{entropy}}(s)} -$$

The entropy appears the good meausre for analyzing the order or disorder of the signal.If the signal is generated with mono-frequency,then it wavelet entropy(WE) will be almost zero as engery is contributed from single frequency at particular level.However if signal is generated from the random processes having muliple frequncies then WE will be signficant at particular level,because different frequencies engery will contribute.The noise signal given in figure 14,15,16,17 extracted from the simulation and operational data is decomposed into six levels.Signal is non-stationary ,so the apparent choise is the wavelet transfrom for the decomposition.

Different wavelet candidates families are available.The only intrest is to calculate the energy of signal at each level,so orthogonality and compact support characterisitics of the wavelet bases are considered.Debauchies,Coiflets and symlets are good candidates for the decomposition of the noise signals given in figures 14,15,16,17 owing to their orthorgonality and compact support characteristic and every family provides good results,however as debauchies 4 is taken into operation.The Db4 has four wavelet and four scaling coefficients.The scaling function coefficients are

$$h1 = \frac{1+\sqrt{3}}{4\sqrt{2}}, h2 = \frac{3+\sqrt{3}}{4\sqrt{2}}, h3 = \frac{3-\sqrt{3}}{4\sqrt{2}}, h4 = \frac{1-\sqrt{3}}{4\sqrt{2}},$$

The scaling function coffients are

$$g1 = \frac{1-\sqrt{3}}{4\sqrt{2}}, g2 = \frac{\sqrt{3}-3}{4\sqrt{2}}, g3 = \frac{3+\sqrt{3}}{4\sqrt{2}}, g4 = \frac{1+\sqrt{3}}{4\sqrt{2}}$$

Six Level decomposition filter banks is given in figure 28,where

h[n] is high pass filter,g[n] is low pass filter, D is detail coefficients ,A is approximate coefficients.The explanation on the functioning of scaling i.e low pass filter g[n] and wavelet i.e. high pass filter h[n] is given in appendix A

The signal x[n] is applied at the input of the filter bank and it is decomposed into six levels.The signal is decomposed into high frequency compoentnes i.e. details and low frequency compoenents i.e. approximations,then at every level approximation is applied again to both high pass filter and low filter to decomposition into high and low frequency components. This process goes on up to six levels. After decomposing the signal into six levels,engery of the each approximation is calculated.The energy of noise signal from blocked and unblocked channels of the sensing system can be partioned at levels.Mathematically it is given as

$$ED_{jk} = \sum_{k=1}^{N} |D_{jk}|^2 \ j = 1, 2, ... l -------(31)$$

$$EA_l = \sum_{k=1}^{N} |A_{jk}|^2 ------(32)$$

$j = 1,2,...l$ is the wavelet decomposition level from level 1 to level l

N is number of samples of detail or approximate at each decomposition level

ED_j is the Engery distribution of detail at decompostion level k

EA_l is the Engery distribution of approximation at decompostion level l

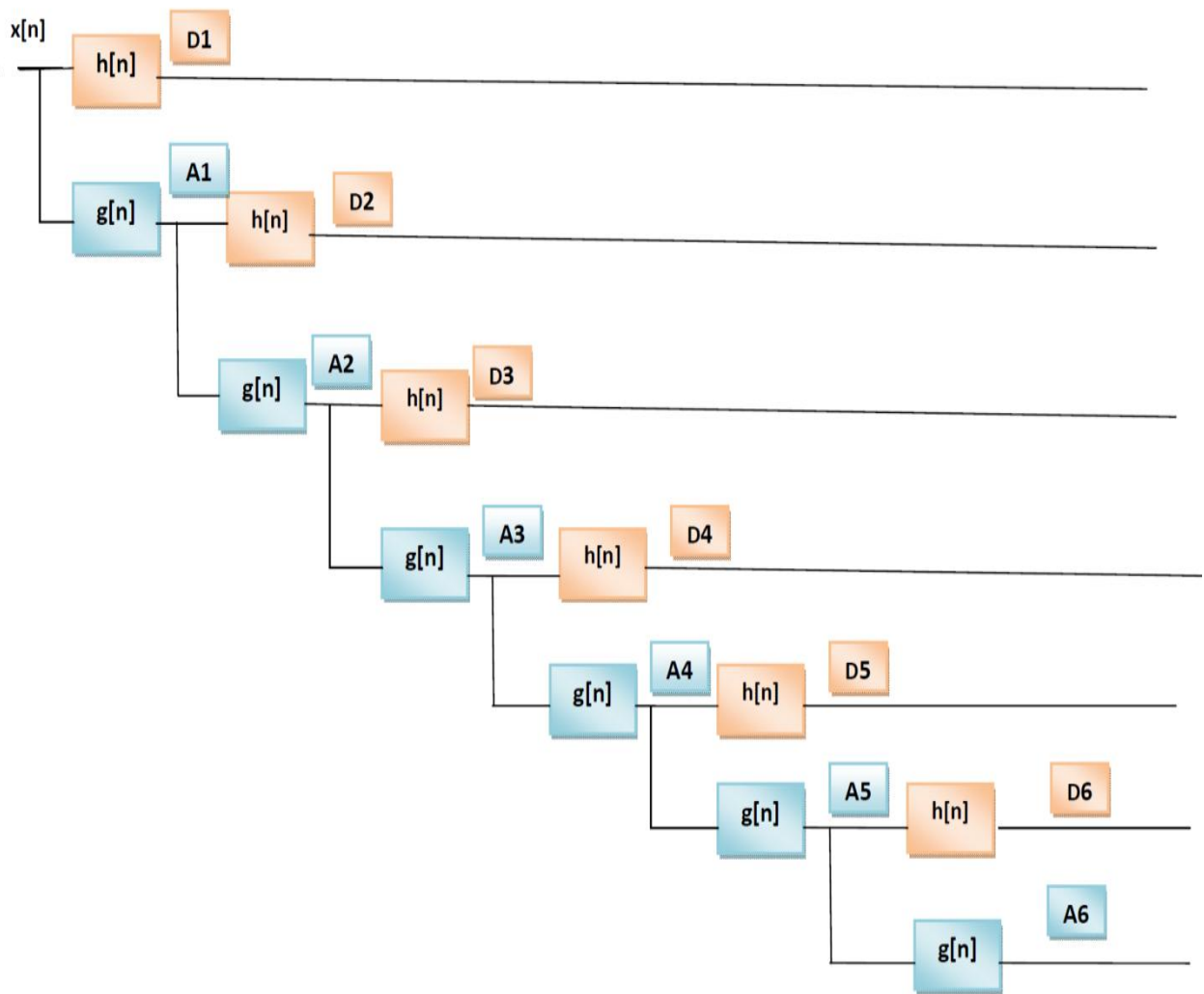Energy disributon is squared summation of wavelet coefficients at level l

Figure 28: Wavelet filter banks for 6th Level Decomposition

4. Results

4.1 Decomposition of Unblocked Channel Operational Noise Signal

Noise signal from unblocked channel of RVLMS is shown figure 16.The noise signal is applied at the input of the wavelet filter banks as shown in figure 28.The signal is decomposed into six levels.The details and approxations are separated.Figure 29 shows the decompositions of the signal .The a1,a2…..a6 are approximations and d1,d2…….d6 are details.The percentage energy distribution at each level is calculated.The bar graph given in figure 30shows the engery of the signal at each level.It is worth mentioning that energy of the low frequency components i.e. i.e.,a1,a2,a3…a6 are calculated.Low frequency components of signal contains the significant part of the energy.It is evident from figure 30 that enegry level is reducing as decomposition. level increases.The percentage of energy at first level is almost 90% however at sixth level it is decreased up to 18%. Each succeeding level has half the number of samples,than the perceding level. Wavelet filter bank given in figure 28, down sample the approximations and details by 1/2 at each level. It means number of samples is halved at each succeeding level and energy is decreasing at each level. Equation 32 suggests,energy is squared summation of the samples at each level.
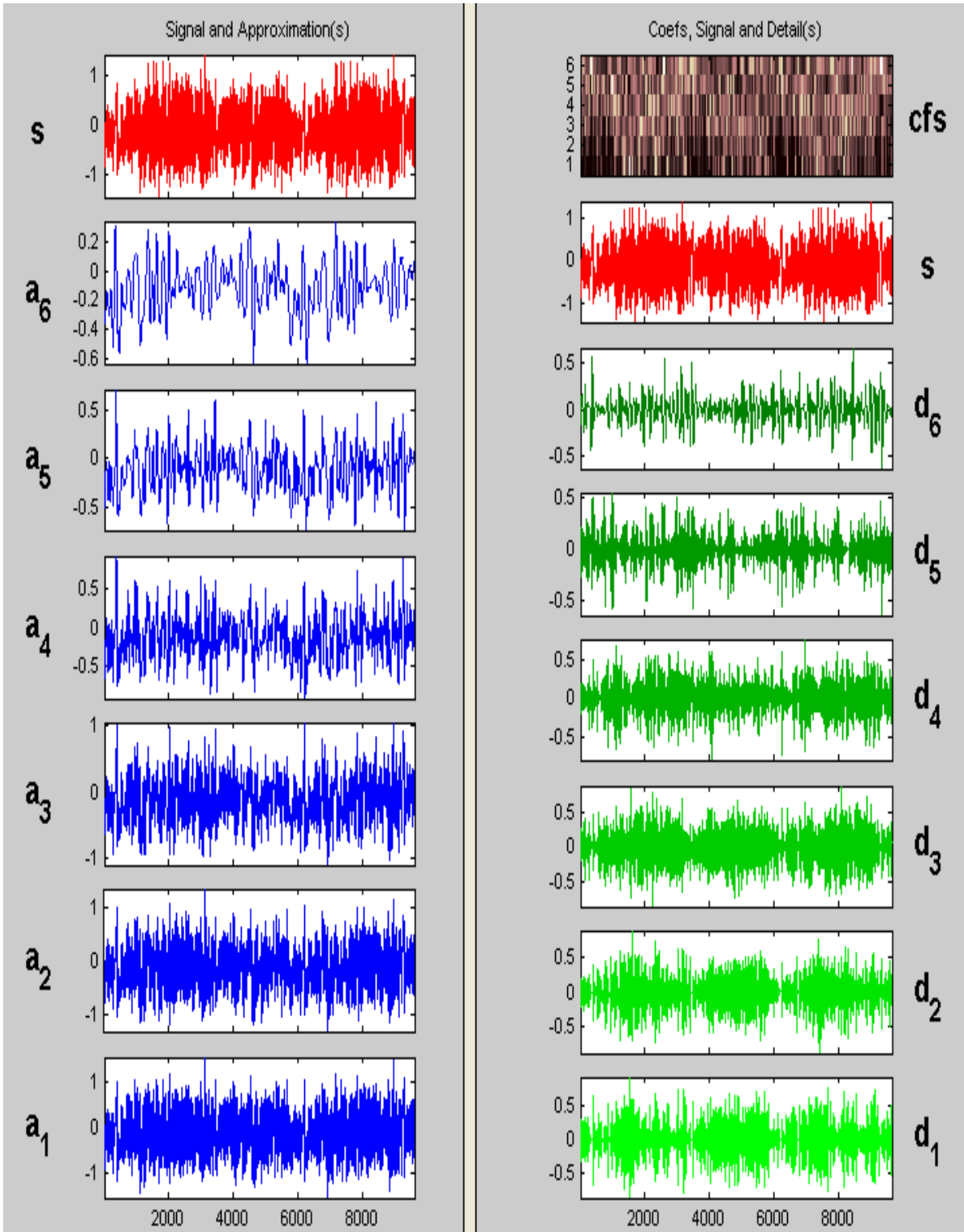
Figure 29: Decomposition of Un-blocked Channel noise signal

Engery Distribution Diagram of Un-Blocked Noise Signal
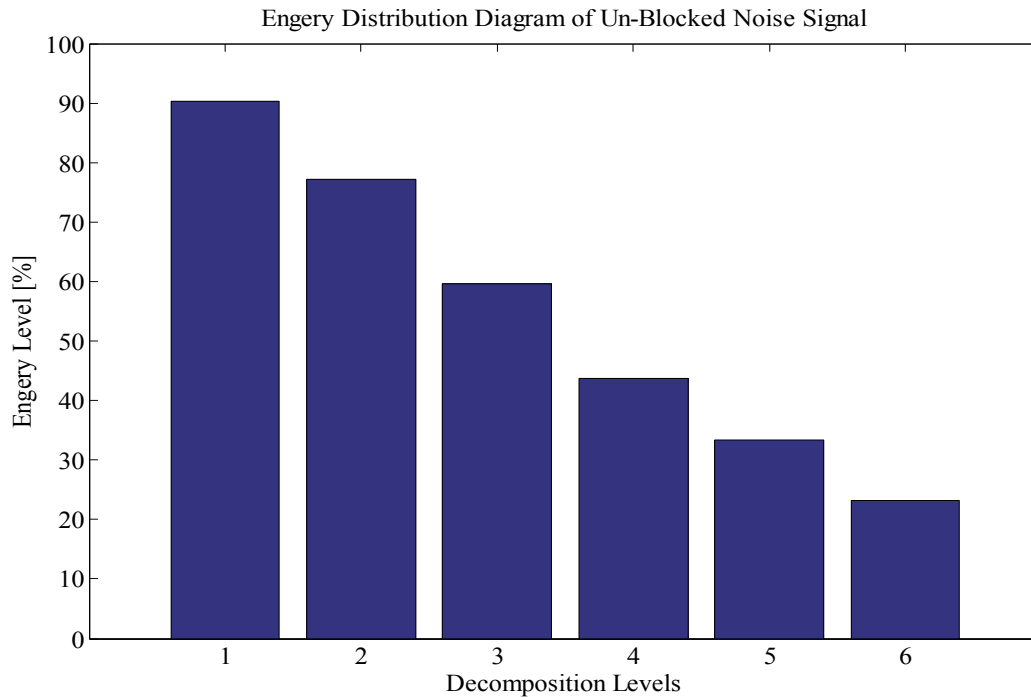
Figure 30: Energy Distribution Diagram of the Un-blocked Noise Signal

4.2 Decomposition of Blocked Channel Operational Noise Signal

The noise signal from blocked channel shown in figure 14 is decomposed in the same way as unblocked channel noise signal. The decomposition into approximations and details is shown in figure 31.The obversation noted is, that amplitude of the approximations is decreased as compared to the approximations of the unblocked channel noise signal,hence engery level is also reduced.The graph of the percentage of energy distribution at each level is shown in figure 32. Comparison between the energy levels of unblocked and blocked channel noise signals is performed to observe the behaviour of energy levels in unblocked and blocked channels.Figure 33 is an overlay graph of the two operational noise signals .It is evident from the figure that engery levels of the blocked noise signal are at reduced amplitude as compared to the unblocked noise signal.
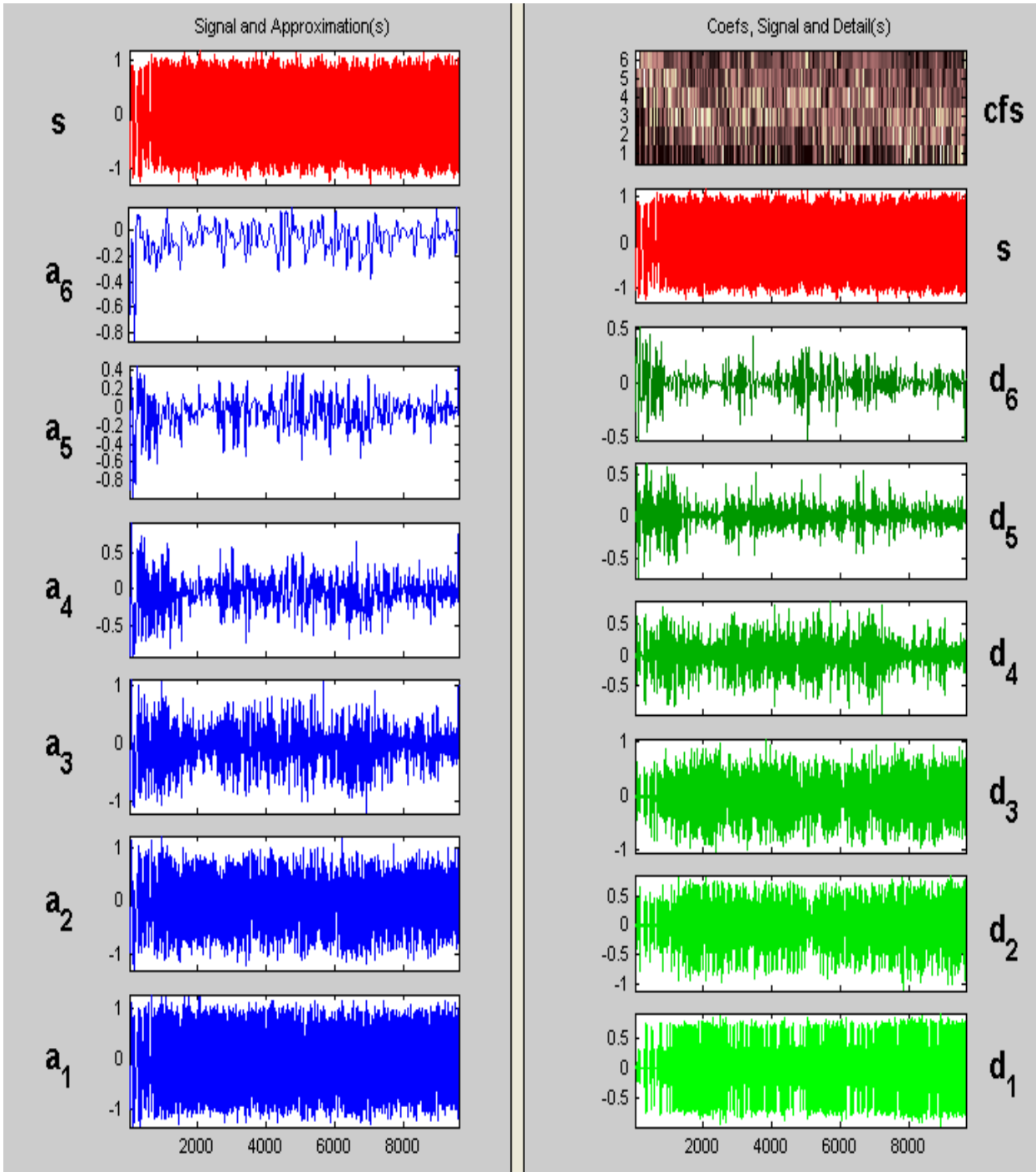
Figure 31: Decomposition of Blocked Channel Noise Signal
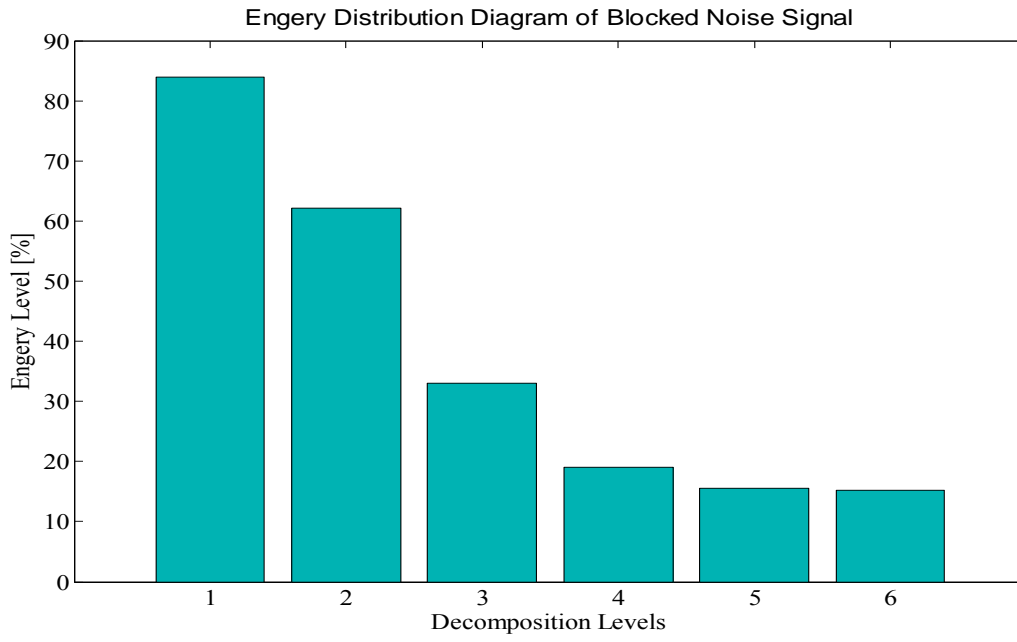
Figure 32: Energy Distribution Diagram of the Blocked Noise Signal.
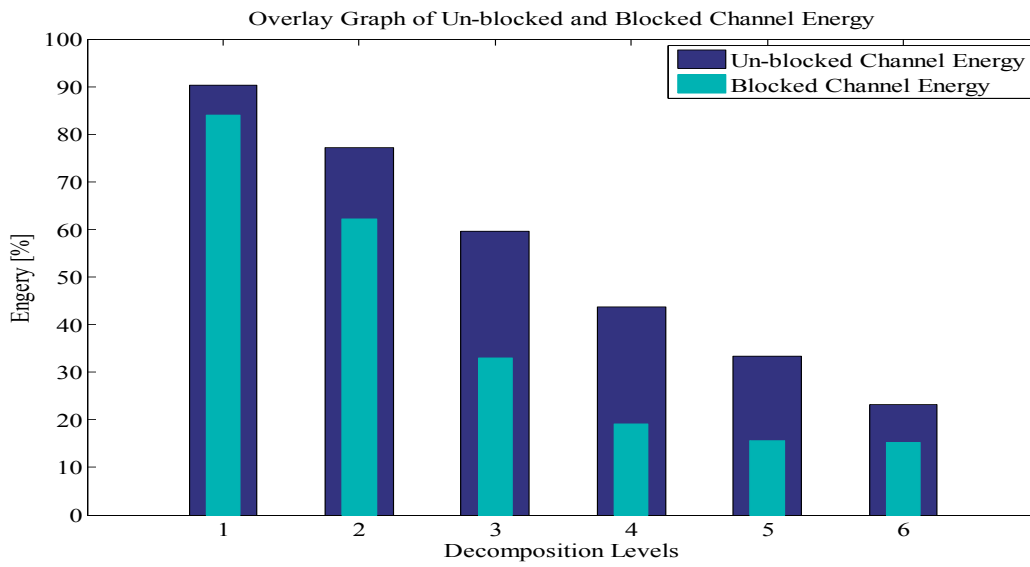
Figure 33: Energy Level Comparison between the Blocked and Un-blocked Noise

Signals

4.3 Decomposition of Un-Blocked Channel Model Noise Signal

The noise is added to the model as shown in figure 34. It is extracted from the model as given in figure 14.The model was not clogged and hence noise signal is from unblocked model.It is done to match the conditions with unblocked channel noise signal i.e. operational data.The intent is to validate the simulation model.Noise signal composed of eight thousands samples is decomposed Noise signal is taken from unblocked channel of RVLMS. Approxmations and details are shown in figure 34.
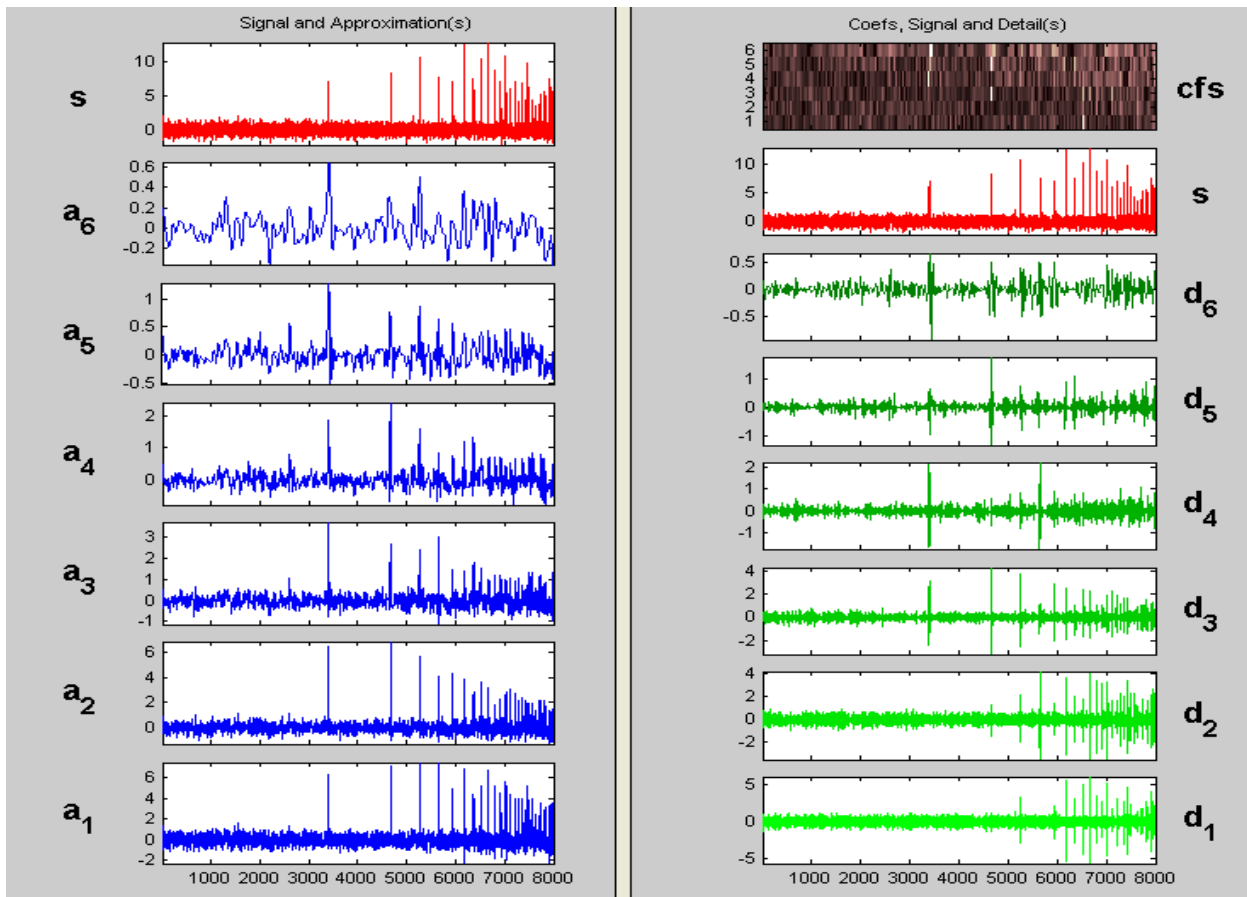
Figure 34: Decomposition of Un-blocked Channel Noise signal (Simulation Model)

Next, the percentage of energy is calculated for approximations at each level. Figure 35shows the energy distribution trend. The percentage of energy at level one is almost 67.78% and at

sixth level is 4.095%.The trend is similar as noted in figure 30.

Energy Distribution Diagram of Un-Blocked Noise Signal(Model)

(Y-axis: Energy Level [%], X-axis: Decomposition Levels)
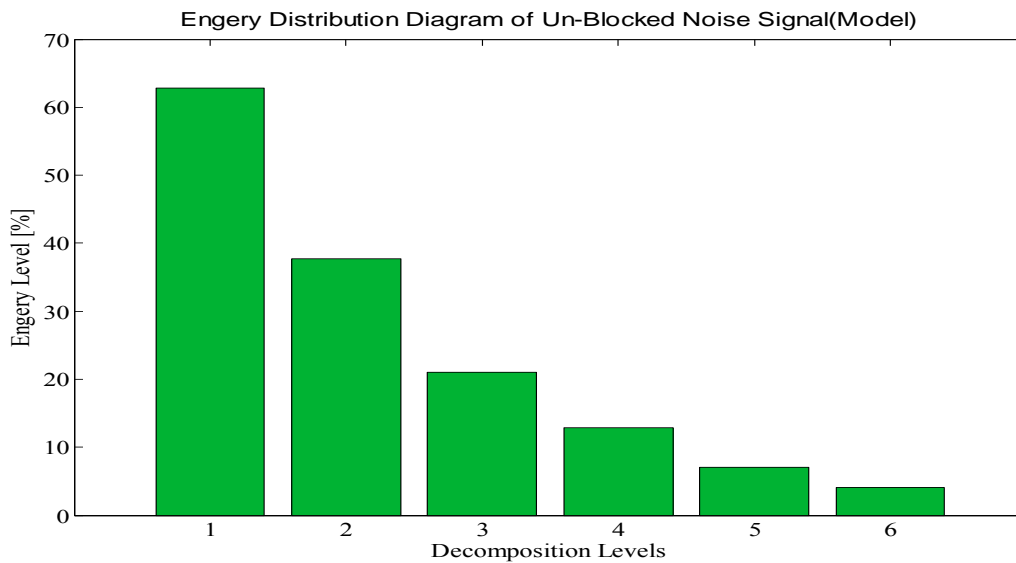
Figure 35: Energy Distribution Diagram of the Un-blocked Noise Signal (Model)

4.4 Decomposition of Blocked Channel Model Noise Signal

The radius of the simulation model is reduced to match the conditions with blocked channel noise signal from the plant. The noise is extracted as given in figure 15.The noise signal is decomposed into approximations and details as previously shown in figure 36. The percentage of energies is calculated and is shown in figure 37.The trend is similar as of operational noise signal from blocked channel. Comparison between the energy levels of unblocked and blocked noise signals shows that energy levels are decreased in blocked channels noises.

Figure 36: Decomposition of Blocked Channel Noise signal (Simulation Model)

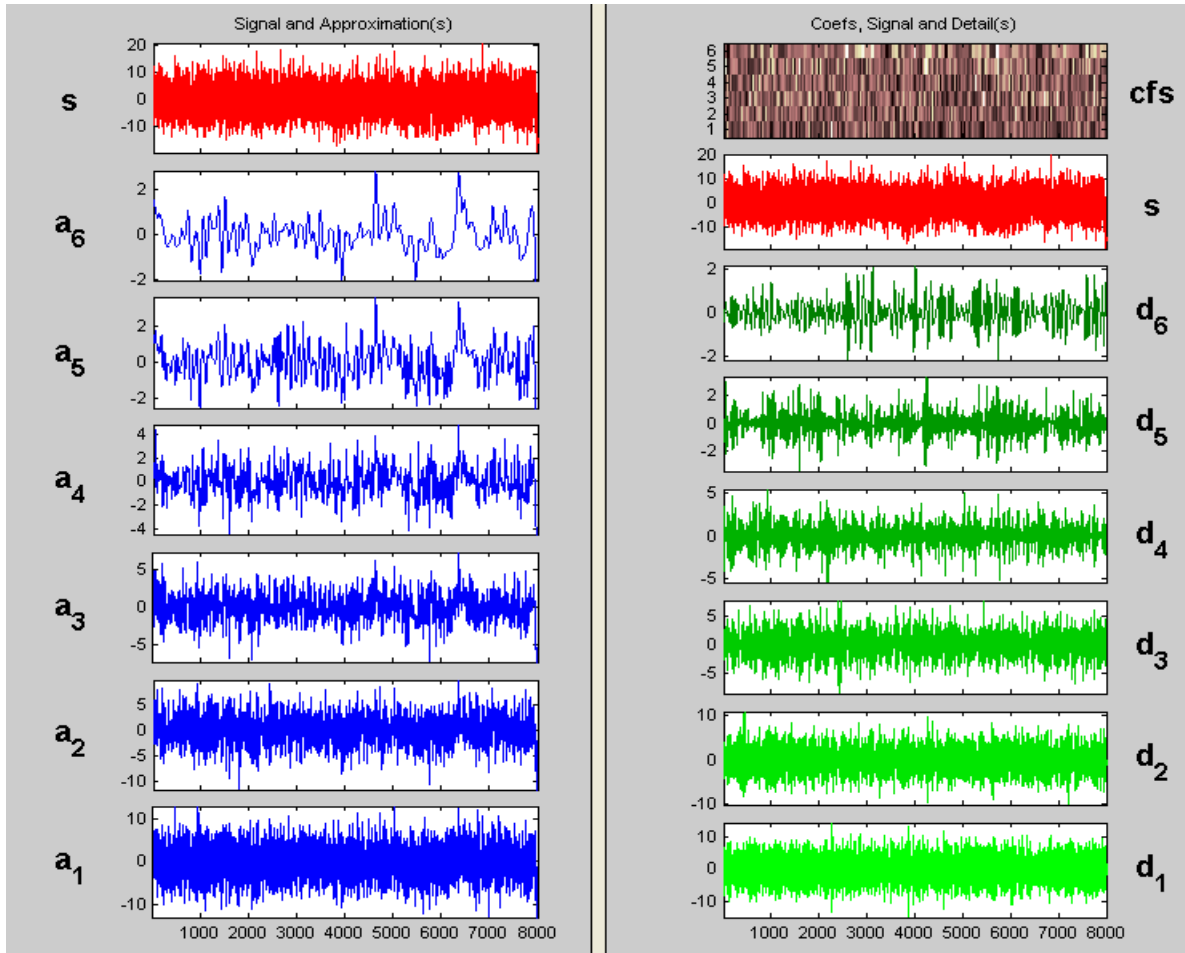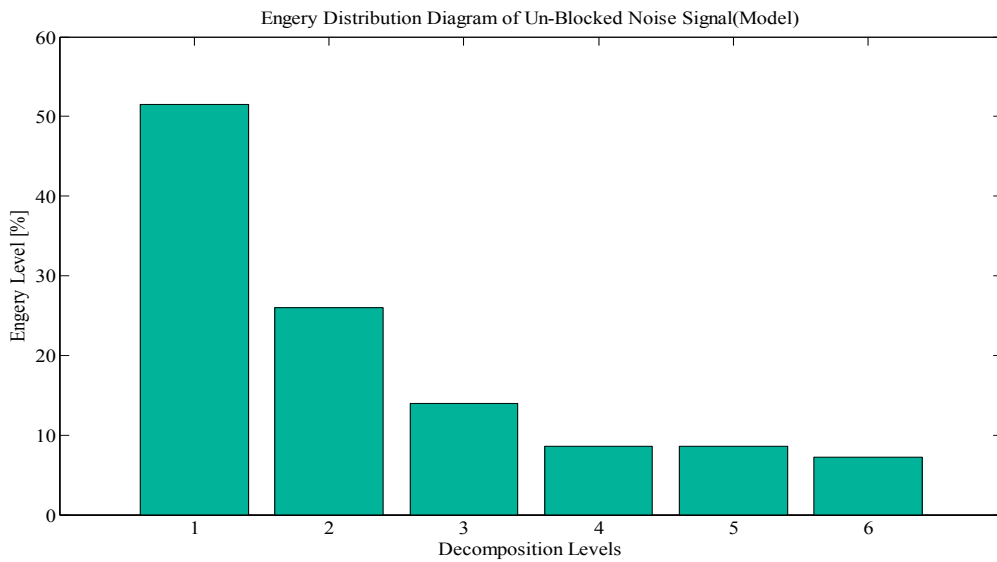**Figure 37: Energy Distribution Diagram of the Blocked Noise Signal (Model)**

49

5. Discussion, Conclusion and Recommendations

5.1 Discussion

Figure 33 shows that as the blockage levels are increased, the signal energies are decreased. Percentage of energies for the blocked channel noise signals are at reduced levels compared to unblocked channel data, this behavior validates the simulations performed in figure 12.As blockages levels are increased by decreasing the radius of the sensing line, the gain of peaks is reduced. Table 3 has documented the results of reductions in peak gain vis-à-vis increments in blockages levels. For example Gain of peak three in normal case is almost

-17dB, in medium and severe blockages, it is almost -51dB and -70dB, respectively.

Figure 33 consolidates simulation behavior i.e.as blockages in sensing lines is increased the energy percentage of noise signal is decreased. The energy percentage at level one of unblocked channel noise signal is at 90.2 and that of blocked channel is at 83.9%.The same behavior is observed at succeeding levels. Thus simulation results as given in figure 12 and operational data results figure 33 are in good agreement. Figure 38, shows comparison between the energies of unblocked channel noise signal from the plant and simulation model. It is clear from the graph that trend is similar; however energy levels of simulation model are at reduced rates as compared to operational data. This could be because operational data has multiple noise sources e.g. Motors may generate electrical noise with multiple harmonics. This may have produced higher noise levels and therefore higher energy levels.

Figure 38: Overlay Graph of Un-Blocked Energy-Operational and Simulation Model
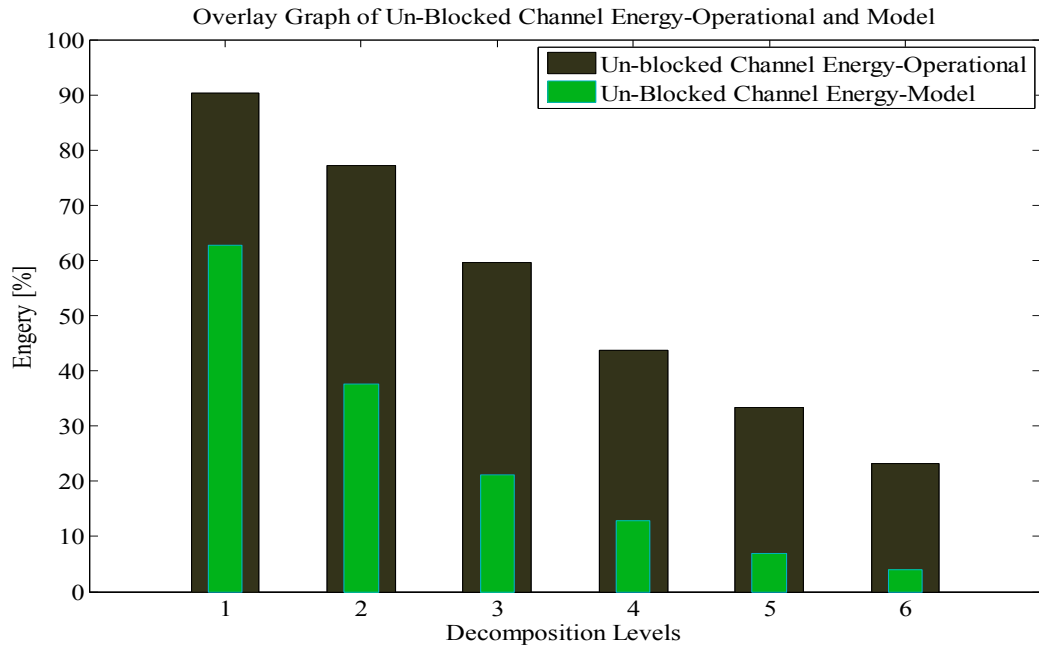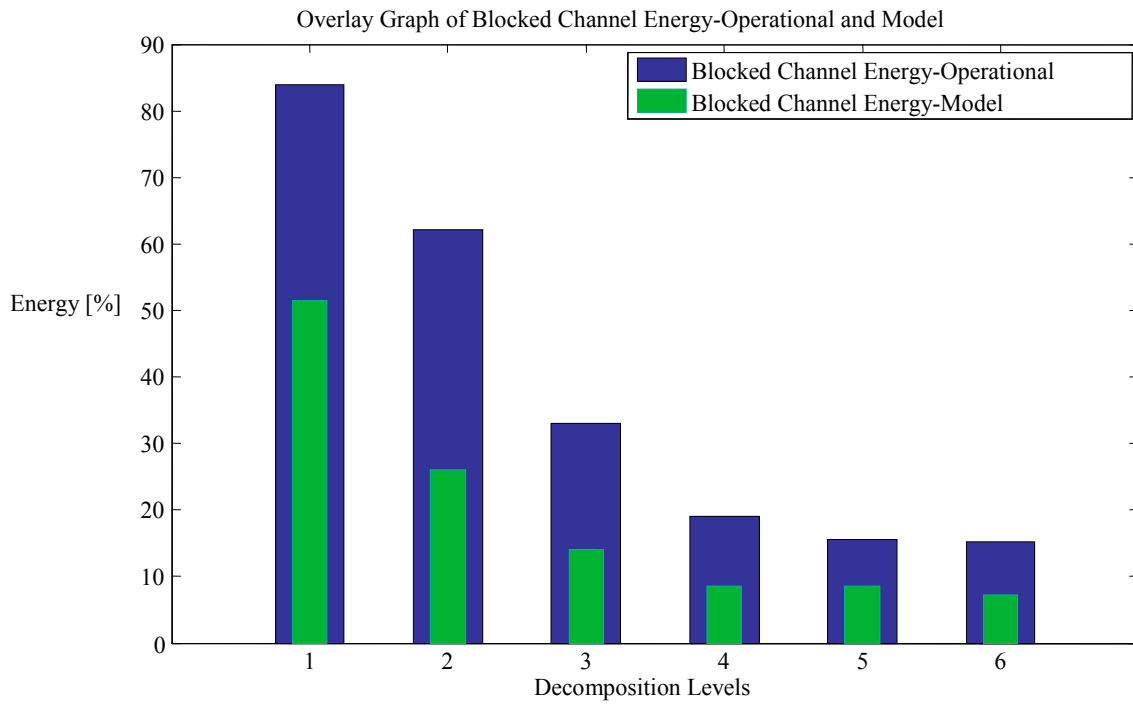

Figure 39: Overlay Graph of Blocked Energy-Operational and Simulation Model

Figure 38 is the comparsion between energy percentages of Un- blocked noise signals from plant and simulation results.It is observed that trend in energy level decrement is similar. Figure 39 shows the engery percentages of blocked noise signals from plant and simulation results. It is clear that these noise signals have also similar trend.as figure 38Therefore we can deduce that simulations and operational data results are consistent.

5.1 Conclusion

The Simulations of sensing lines blockages of the Nuclear Power plant are successfully carried out. Equivalent Pi circuit is used for modeling of the level sensing line using electrical-hydraulic analogies. The data from the nuclear power plant is utilized to compare with the simulations. The results show good consistency. According to simulation results as blockages are increased, the transfer function gain of the resonant peaks is reduced. The operational data results flank the simulation behavior i.e.as blockage level is increased the percentage energy levels is decreased. Thus in our opinion variation in energy levels can be used as the indicator for the on line monitoring of the sensing lines.

5.2 Future Recommendations

Energy distribution at decomposed levels of model and plant noise signal shows good consistency. In my opinion Artificial Neural Network (ANN) can be developed to monitor the health of the sensing line based on the classification of the energies. Extensive regulations upon nuclear power plant design require safety related equipment to be qualified according to prevailing standards. ANN also needs to be qualified as per nuclear safety standards before their applications in nuclear power plants. It is recommended that future research may be carried out upon the qualification of hard ware of filter banks and ANN according to nuclear industry standards.

Periodgoramof Unblocked Noise Signal-Operational
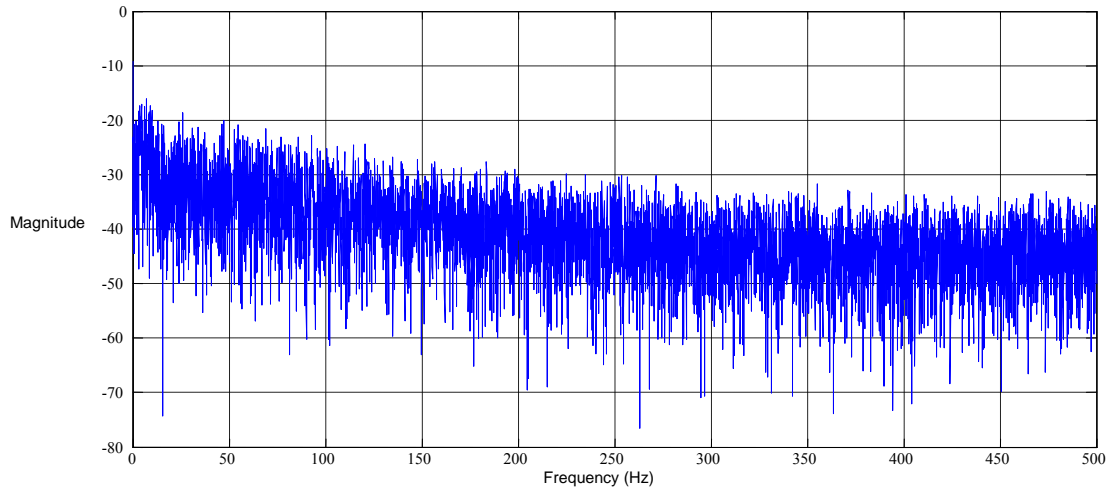
(a) Periodogram of unblocked noise Signal-operational

Periodogram of the Blocked Noise Signal-Operational
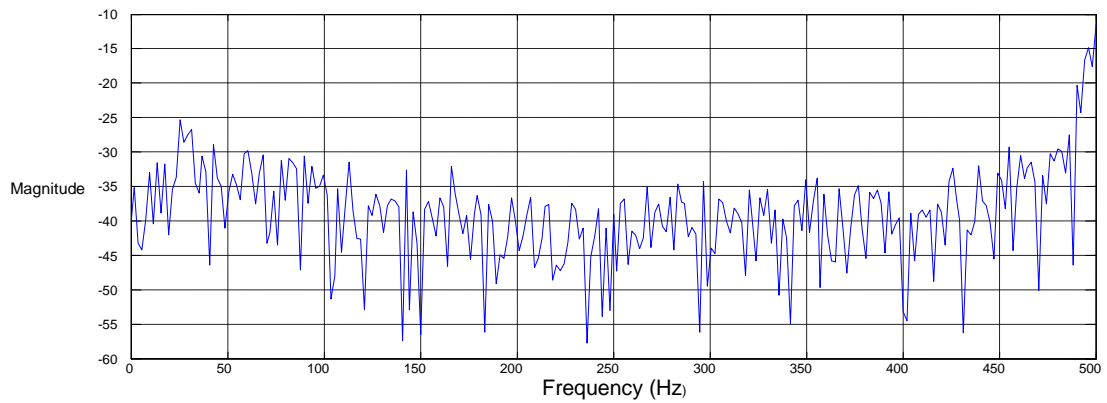
(b) Periodogram of Blocked noise Signal-operational

Figure 40: Periodogram of unblocked and Blocked Channel Noise Signal-Operational

Appendix

This appendix provides the equations and their explanations for decompositions of the signal with Haar and daubechies wavelet transforms. The signal coefficients are taken from the unblocked noise signal. The signals are decomposed up to six levels using the wavemenu function of the MATLAB. The appendix provides the descriptions how window function slides upon the signal and how coefficients of the low frequency and high frequency components are achieved.

Haar Wavelet Transform

All the wavelet transforms decomposes the signal into high frequency and low frequency components. Haar wavelet is doing the same job i.e. decomposes the signal into two sub bands. One sub band is called high frequency or details and other is called low frequency or approximations.`

Let's see how to calculate the approximations or low frequency components. First low frequency signal $a^1 = (a_1, a_2, a_3, \ldots\ldots)$ is computed by taking the running average as follows.

$$a_1 = \frac{f_1 + f_2}{\sqrt{2}}$$

Similarly the next value is taken as

$$a_2 = \frac{f_3 + f_4}{\sqrt{2}}$$

The process will go on and all the values of a's will be calculated. These values are the output coefficients of the low pass filter. Which is approximation (A) of the filter bank given in figure 28.

A precise formula for calculating the low frequency components are given as

$$a_n = \frac{f_{2n} - 1 + f_{2n}}{\sqrt{2}} - - - - - (a)$$

For n=1,2,3,4……….N/2

For example we have taken first eight values of our unblocked noise signals given as f and calculate the coefficients for low frequency signal,

f= (0.386, 1.009, 0.9456, 0.821, 0.4239, 0.1333, 0.773, 0.340)

Using the equation (a), first low frequency signal is calculated as

$$a^1 = (0.986, 1.24, 0.393, 0.758)$$

Other sub band signal is details (d_m) or high frequency components

Details can be calculated using the running difference as

$$d_m = \frac{f_{2m} - 1 + f_{2m}}{\sqrt{2}} - - - - - (b)$$

Using the coefficients of the unblocked noise signals, we calculate the first high frequency c signal as follows,

$$d^1 = (-0.446, 0.087, 0.211, 0.306)$$

The haar transform can be performed up to many levels, however we have decomposed the signal up to six levels, so low frequency components are decomposed up to A6,and high frequency will go up to D6.

Another important property, we explained in chapter 4 is that, low frequency components, have more energy as compared to high frequency components. By the energy of the signal we mean, the sum of square of its values

So energy in $a^1 = (0.986^2 + 1.24^2 + 0.393^2 + 0.758^2) = 3.23$, and energy in

$d^1 = ((-0.446)^2 + 0.087^2 + 0.211^2 + 0.306^2) = 0.344$

Hence we can say that approximations contain more energy as compared to details, that's why we have chosen the former for the indication.

Daubechies Wavelet Transform

The Daubechies wavelet transforms are explained in the same way as is Haar wavelet transform by calculating running averages and differences by using scalar products with scaling and wavelets functions. There are many variations of the Daubechies signal e.g.Db1,Db2,Db3 etc. We used db4 for our signals decomposition.

The Db4 wavelet transform is defined in essentially the same way as the Haar wavelet transform. If a signal f has an even number N of values, then the 1-level Db4 transform is the dividing the signal into its first approximation sub signal a_1 and first detail sub signal d_1.

Each value a_m of $a_1 = (a_1,..., a_{N/2})$ is equal to a scalar product:

$$a_m = f \cdot V^1{}_m \quad \text{-----------------(c)}$$

Likewise, each value d_m of $d_1 = (d_1,..., d_{N/2})$ is equal to a scalar product:

$$d_m = f \cdot W^1{}_m \text{--------------------(b)}$$

The difference between the Haar transform and the Daub4 transform lies in the way that the scaling signals and wavelets are defined. We shall first discuss the scaling signals. The scaling numbers h_1, h_2, h_3, h_4 be defined as,

$$h_1 = 1 + \sqrt{3}/ (4 \sqrt{2}) ,$$

$$h_2 = 3 + \sqrt{3}/(4 \sqrt{2}) ,$$

$$h_3 = 3 - \sqrt{3} /(4 \sqrt{2}),$$

$$h_4 = 1 - \sqrt{3}/(4 \sqrt{2})$$

Using these scaling numbers, the 1-level Daub4 scaling signals are

$$V^1_{\ 1} = (h_1, h_2, h_3, h_4, 0, 0... 0)$$

$$V^1_{\ 2} = (0, 0, h_1, h_2, h_3, h_4, 0, 0... 0)$$

$$V^1_{\ 3} = (0, 0, 0, 0, h_1, h_2, h_3, h_4, 0, 0... 0) \text{ and so on}$$

These scaling signals are closely related to each other. For example, each scaling signal has a support of four time-units. Also observe that the second scaling signal $V^1_{\ 2}$ is translation of the first scaling signal $V^1_{\ 1}$ by two time-units. In the same way the third scaling signal $V^1_{\ 3}$ is a translation by four time-units of $V^1_{\ 1}$, and each subsequent scaling signal is a translation by a multiple of two time-units of $V^1_{\ 1}$. This process will go on.

Here we will discuss the Db4 wavelets. Let the wavelet numbers g_1, g_2, g_3, g_4 be defined by

$$g_1 = 1 - \sqrt{3} /(4 \sqrt{2})$$
$$g_2 = \sqrt{3} - 3 /(4 \sqrt{2})$$
$$g_3 = 3 + \sqrt{3} (4 \sqrt{2})$$
$$g_4 = -1 - \sqrt{3}/ (4 \sqrt{2})$$

Notice that the wavelet numbers are related to the scaling numbers by the equations:

$$g_1 = h_4$$

$$g_2 = -h_3$$

$$g_3 = h_2$$

$$h_4 = -h_1$$

The wavelets translations are defined as follows

$$W^1{}_1 = (g_1, g_2, g_3, g_4, 0, 0,... , 0)$$

$$W^1{}_2 = (0, 0, g_1, g_2, g_3, g_4, 0, 0,... , 0)$$

$$W^1{}_3 = (0, 0, 0, 0, g_1, g_2, g_3, g_4, 0, 0,... , 0) \ . . . \text{ and so on}$$

These wavelets are all translates of $W^1{}_1$,

Daubechies 4 has following Scaling function equation

$$a[i]=h_1s[2i]+h_2s[2i+1]+h_3s[2i+2]+h_4s[2i+3]\text{----------(d)}$$

We have taken the eight coefficients of our signal as our function space and it is given as

f=(0.386,1.009,0.9456,0.821,0.4239,0.1333,0.773,0.340),we take

s_1=0.386,s_2=1.009,s_3=0.9456,s_4,=0.821,s_5=0.4239,s_6=0.1333,s_7=0.773,s_8=0.340

Expanding the scaling equation (d) gives us

$$a[1]= h_1s[2]+h_2s[3]+h_3s[4]+h_4s[5]\text{---------------------------(e)}$$

Putting values of h_1 to h_4 and s_1 to s_4 gives us

a[1]= [1 + √3/ (4 √2)(1.009)]+ 3 + [√3/(4 √2)(0.9456)]+ [3 − √3 /(4 √2) (0.821)]+[1 − √3/(4 √2)(0.4239)

Similarly a[2] is calculated using equation (f)

$$a[2]= h_1 s[4]+h_2 s[5]+h_3 s[6]+h_4 s[7] \text{------------------------------(f)}$$

a[2]=[1 + √3/ (4 √2)(0.821)]+ 3 + [√3/(4 √2)(0.4239)]+ [3 − √3 /(4 √2) (0.9456)]+[1 − √3/(4 √2)(0.773)

a[3] is calculated by equation (g)

$$a[3]= h_1 s[6]+h_2 s[7]+h_3 s[8]+h_4 [s9] \text{----------------------------(g)}$$

a[3]=[1 + √3/ (4 √2)(0.1333)]+ 3 + [√3/(4 √2)(0.773)]+ [3 − √3 /(4 √2) (0.340)]+[1 − √3/(4 √2)s[9]]

The equations (e) to (g) verify that function is sliding upon the function space and function has support of four units. The sliding window is translation of two units than previous one. Wavelet function is given as follows

$$d[i]=g_1 s[2i]+g_2 s[2i+1]+g_3 s[2i+2]+g_4 s[2i+3] \text{------------------------(h)}$$

for d_1, replace i=1

$$d[1]= g_1 s[2]+g_2 s[3]+g_3 s[4]+g_4 s[5]$$

Putting the values of g1 to g4 and s1 to s4 gives us

d[1]= [(1 − √3 /(4 √2)(1.009)]+ [(√3 − 3 /(4 √2)(0.9456)]+ [(3 + √3 (4 √2)(0.821)]

+[(−1 − √3/ (4 √2)(0.4239)

59

The window slides two units forward and d[2] is obtained as

$$d[2] = g_1 s[4] + g_2 s[5] + g_3 s[6] + g_4 s[7] \text{---------------------------------(i)}$$

Putting the values of g_1 and signal coefficients we get

$$d[2] = [(1 - \sqrt{3}/(4\sqrt{2})(0.821)] + [(\sqrt{3} - 3/(4\sqrt{2})(0.4239)][(3 + \sqrt{3}(4\sqrt{2})(0.1333)] +$$

$$[(-1 - \sqrt{3}/(4\sqrt{2})(0.4239)]$$

Window is translated two units more and the d [3] is obtained as follows,

$$d[3] = g_1 s[6] + g_2 s[7] + g_3 s[8] + g_4 s[9] \text{-----------------------------------(j)}$$

$$d[3] = [(1 - \sqrt{3}/(4\sqrt{2})(0.1333)] + [(\sqrt{3} - 3/(4\sqrt{2})(0.773)][(3 + \sqrt{3}(4\sqrt{2})(0.340)] +$$

$$[(-1 - \sqrt{3}/(4\sqrt{2})(s9)]$$

The equations (i) to (j) verify that function is sliding upon the function space and function has support of four units. The sliding window is translation of two units than previous one. The d's are the high frequency components.

References

[1] J. Vujić, R. M. Bergmann, R. Škoda, and M. Miletić, "Small modular reactors: Simpler, safer, cheaper?," *Energy*, vol. 45, pp. 288–295, 2012.

[2] H. M. Hashemian, "On-line Monitoring and Calibration Techniques in Nuclear Power Plants.",IAEA-CN-164-7S05

[3] K. Lin and K. E. Holbert, "Void diagnostics in liquid-filled pressure sensing lines," *Prog. Nucl. Energy*, vol. 52, no. 5, pp. 503–511, 2010.

[4] H. M. Hashemian, J. a. Thie, B. R. Upadhyaya, and K. E. Holbert, "Sensor response time monitoring using noise analysis," *Prog. Nucl. Energy*, vol. 21, no. 2, pp. 583–592, 1988.

[5] H. M. Hashemian and J. Jiang, "Using the noise analysis technique to detect response time problems in the sensing lines of nuclear plant pressure transmitters," *Prog. Nucl. Energy*, vol. 52, no. 4, pp. 367–373, 2010.

[6] N. L. T. Lile, M. H. M. Jaafar, M. R. Roslan, and M. S. M. Azmi, "Blockage Detection in Circular Pipe Using Vibration Analysis," *Int. J. Adv. Sci. Eng. Inf. Technol.*, vol. 2, no. 3, pp. 54–57, 2012.

[7] J. Barbero and J. Bla, "Transmitters : the Shift of Spectrum Resonances," vol. 199, pp. 327–334, 2000.

[8] H. M. Hashemian and J. Jiang, "A practical review of methods for measuring the dynamic characteristics of industrial pressure transmitters," *ISA Trans.*, vol. 49, no. 1, pp. 2–9, 2010.

[9] C. Montalvo, a. García-Berrocal, J. Blázquez, and M. Balbás, "The Hilbert transform as a quality control tool in capacitive pressure transmitters," *Mech. Syst. Signal Process.*, vol. 24, pp. 1025–1031, 2010.

[10] a. García-Berrocal, J. M. Chicharro, J. Blázquez, and M. Balbás, "Non-linear noise analysis from a capacitive pressure transmitter," *Mech. Syst. Signal Process.*, vol. 18, pp. 187–197, 2004.

[11] D. Ozevin and J. Harding, "Novel leak localization in pressurized pipeline networks using acoustic emission and geometric connectivity," *Int. J. Press. Vessel. Pip.*, vol. 92, pp. 63–69, 2012.

[12] A. K. M. F. Haque, M. H. Ali, M. A. Kiber, and M. T. Hasan, "Detection of small variations of ECG features using wavelet," *J. Eng. Appl. Sci.*, vol. 4, no. 6, pp. 27–30, 2009.

[13] K. Lin and K. Holbert, "Pressure sensing line diagnostics in nuclear power plants," *Nucl. Power*, pp. 97–123, 2010.

[14] D. Matko, G. Geiger, and W. Gregoritza, "Pipeline simulation techniques," *Math. Comput. Simul.*, vol. 52, pp. 211–230, 2000.

[15] H. Saadat, *Power System Analysis*. ,Third Edition,2010.

[16] *"DOE fundamentals Handbook Instrumentation and Control Volume 1 of 2,"* *Control*, vol. 1, no. June, 1992.

[17] P. S. Addison, *The Illustrated Wavelet Transform Handbook: Applications in Science, Engineering, Medicine and Finance*. 2002.

[18] S. Mallat, "A Wavelet Tour of Signal Processing," *A Wavelet Tour Signal Process.*, pp. 20–41, 1999.

[19] M. Weeks, *Digital signal processing using matlab and wavelets*. 2007, p. 768.

[20] K. Lin and K. E. Holbert, "Blockage diagnostics for nuclear power plant pressure transmitter sensing lines," *Nucl. Eng. Des.*, vol. 239, pp. 365–372, 2009.

[21] M. Misiti and Y. Misiti, "Wavelet toolbox," *MathWorks Inc., …*, 1996.

[22] K. Bartecki, "A transfer function representation for a class of hyperbolic systems," *2012 17th Int. Conf. Methods Model. Autom. Robot. MMAR 2012*, no. 3, pp. 611–616, 2012.

[23] O. Begovich, a. Navarro, E. N. Sánchez, and G. Besançon, "Comparison of two detection algorithms for pipeline leaks," *Proc. IEEE Int. Conf. Control Appl.*, no. October, pp. 777–782, 2007.

[24] M. Behbahani-Nejad and a. Bagheri, "The accuracy and efficiency of a MATLAB-Simulink library for transient flow simulation of gas pipelines and networks," *J. Pet. Sci. Eng.*, vol. 70, pp. 256–265, 2010.

[25] J. Bird, "Electrical circuit theory and technology," *Zhurnal Eksp. i Teor. Fiz.*, 2010.

[26] J. Blázquez and J. Ballestrín, "Pressure transmitter surveillance: The dominant real pole case," *Prog. Nucl. Energy*, vol. 29, no. 3, pp. 139–145, 1995.

[27] J. J. Buccafusco and R. S. Aronstam, "Precursors of cholinergic false transmitters: central effects on blood pressure and direct interactions with cholinergic receptors.," *Neuropharmacology*, vol. 27, no. 3, pp. 227–233, 1988.

[28] M. Caresana, a. Denker, a. Esposito, M. Ferrarini, N. Golnik, E. Hohmann, a. Leuschner, M. Luszik-Bhadra, G. Manessi, S. Mayer, K. Ott, J. Röhrich, M. Silari, F. Trompier, M. Volnhals, and M. Wielunski, "Intercomparison of radiation protection instrumentation in a pulsed neutron field," *Nucl. Instruments Methods Phys. Res. Sect. A Accel. Spectrometers, Detect. Assoc. Equip.*, vol. 737, pp. 203–213, 2014.

[29] J. M. Chicharro, a. García-Berrocal, M. Balbás, and J. BLAzquez, "Pressure Transmitter Surveillance Using Quaternion Numbers," *Mech. Syst. Signal Process.*, vol. 16, pp. 1083–1091, 2002.

[30] Y. C. Choi, J. H. Park, and K. S. Choi, "An impact source localization technique for a nuclear power plant by using sensors of different types," *ISA Trans.*, vol. 50, no. 1, pp. 111–118, 2011.

[31] C. Demazière and I. Pázsit, "Numerical tools applied to power reactor noise analysis," *Prog. Nucl. Energy*, vol. 51, pp. 67–81, 2009.

[32] D. Ernesto, T. Romero, and G. J. Dolecek, "Digital FIR Hilbert Transformers : Fundamentals and Efficient Design Methods," *MATLAB – A Fundam. Tool Sci. Comput. Eng. Appl.*, pp. 445–482, 2012.

[33] P. Filliatre, C. Jammes, J. P. Jeannot, and F. Jadot, "In vessel detection of delayed neutron emitters from clad failure in sodium cooled nuclear reactors: Information treatment," *Ann. Nucl. Energy*, vol. 65, pp. 385–389, 2014.

[34] P. Flandrin and O. Lemoine, "Time-Frequency Toolbox," *Recherche*, pp. 1995–1996, 1996.

[35] G. Geiger and D. Matko, "Models of Pipelines in Transient Mode," *Math. Comput. Model. Dyn. Syst.*, vol. 8, no. May 2014, pp. 117–136, 2002.

[36] M. Y. Gokhale, "Time Domain Signal Analysis Using Wavelet Packet Decomposition Approach," *Int'l J. Commun. Netw. Syst. Sci.*, vol. 03, no. March, pp. 321–329, 2010.

[37] V. O. Golubinskaya, O. S. Tarasova, A. S. Borovik, and I. M. Rodionov, "Frequency characteristics of blood pressure oscillations evoked by sympathetic transmitters, noradrenaline and adenosine triphosphate," *J. Auton. Nerv. Syst.*, vol. 77, pp. 13–20, 1999.

[38] D. Wang, D. Miao, and C. Xie, "Best basis-based wavelet packet entropy feature extraction and hierarchical EEG classification for epileptic detection," *Expert Syst. Appl.*, vol. 38, no. 11, pp. 14314–14320, 2011.

[39] Z. K. Peng and F. L. Chu, "Application of the wavelet transform in machine condition monitoring and fault diagnostics: A review with bibliography," *Mech. Syst. Signal Process.*, vol. 18, pp. 199–221, 2004.

[40] a Mertins, *Signal analysis Wavelets, Filtre Banks, Time-Frequency Transforms and Aplications*. 1999.

[41] S. Ouadfeul, L. Aliouane, M. Hamoudi, A. Boudella, and S. Eladj, "1D Wavelet Transform and Geosciences," 2011.

[42] I. Omerhodzic, S. Avdakovic, K. Dizdarevic, and K. Rotim, "Energy Distribution of EEG Signal Components by Wavelet Transform," 2007.

[43] "Time Frequency Analysis for Biomedical Engineering", Chia- Jung Chang ,National Taiwan University